

CHALMERS



A bubble curtain model applied in chlorate electrolysis

Master of Science Thesis in the Master Degree Program, Chemical Engineering

DE STRYCKER, Yannick

Department of Chemistry and Bioscience

Division of Chemical Engineering

CHALMERS UNIVERSITY OF TECHNOLOGY

Göteborg, Sweden, 2012



Artesis Hogeschool Antwerpen

Industriële Wetenschappen: Chemie

Abstract

Sodium chlorate is needed in the pulp and paper industry as a bleaching chemical. The chlorate process requires a high power consumption which implies high electricity costs. Lowering this power consumption requires redesign of electrodes and a better understanding of the hydrogen bubbles that are being formed as a by-product. These bubbles lead to an increased cell voltage which is one of the major issues. In this work hydrogen bubbles are studied, both theoretically and experimentally with respect to formation, growth and collapse and the effect on the cell voltage.

It can be concluded that in general bubbles evenly distributed in the cell gap may contribute with about 0,01 V. The bubble curtain at the cathode accounts approximately for an extra 0,02 V. If a fraction of the cathode is covered by hydrogen bubbles this will increase the voltage with about 0,07 V for a 50% coverage. These values account for a current density of 2000 A/m².

Initial bubble sizes depend on mass transfer and direct bubble formation on the electrode. If the bubble formation is low, the hydrogen concentration will be high which theoretically accomplishes bubbles as small as $3,2 \cdot 10^{-9} m$. The life time of a 1 μm bubble in the vicinity of a 0,1 mm bubble is 0,0042 s which is very small compared with the residence time of electrolyte in the electrode gap of 1 s.

Experimental work was made to find a maximum gas holdup. Hydrogen bubbles were generated under industrial relevant conditions in a small setup. The bubbles were collected in a thin riser tube which made gas voidages easy measurable. The gas voidages may be as high as 0,57 at a superficial gas velocity of 0,0065 m/s and this occurs when the bubble density gets so close packed that bubbles start to coalesce. Different amounts of electrolyte will give different voidages in the experimental setup used. The bubble beds were not stable. Extremely large bubbles of millimeter size were seen. There was coalescence on the walls that disturbed the natural coalescence taking place in the dispersion.

It is proposed to make the converging walls of the inner vessel longer so that the converging part is less steep in order to prevent coalescence. Experimental breakdown occurred due to heat production at the current feeders which made the bottom of the setup melt. Making the current feeders thicker will lower the amount of heat produced. Applying an isolator between the current feeders and the plastic bottom will also reduce the risk of a melting bottom.

Acknowledgements

Thank you Johan for guiding me through this thesis. Even when things did not go that well you still gave me the support I needed. Also thank you for the many times you spoke Swedish with me.

Thank you Bengt for giving your own insights into the matter of this thesis. The conversations we had helped me a lot. The CFD course was given very well and the book was even better. Still, I will never be a big fan of CFD, please don't take this personal ;-)

Thank you Tom for arranging all the necessary things that made it possible for me to experience half a year of studies in Sweden. Without your efforts and the approval of Artesis staff it wouldn't have been possible to learn myself Swedish. I was also very glad you took the time to comment my writings.

I really appreciate the efforts many of the colleagues did to improve my Swedish. All the hours you spent speaking Swedish to me made me happy time after time! Ficka was for me the ultimate moment to learn the language. I can only hope to end up in such a calm and relaxing work environment after my studies.

I would like to thank my roommates Emma, Claudia, Pia, Hanna, Micha, Benno, François, Thibault, Alex, Baptiste, Maxime and Anna Paulson for bringing some joy into my life in Sweden that wasn't particularly the best time I've ever had. Coming home day after day in room filled with joy and happiness meant more for me than you will ever know.

Thank you mom and dad, not for helping with my thesis, but for giving me the best youth one could imagine.

Thank you Irmin, for still being there and to encourage me in the past months.

Table of contents

<i>Chapter 1.</i>	Introduction	1
<i>Chapter 2.</i>	Chlorate cell	2
2.1	Wanted reactions	2
2.2	Parasitic reactions.....	2
<i>Chapter 3.</i>	Goal	3
<i>Chapter 4.</i>	Two-phase flow in an electrode gap.....	4
4.1	Chlorate electrolyte	4
4.2	Hydrogen formation and superficial gas velocity	6
4.3	Bubble formation	8
4.4	Concentration boundary layer and minimum bubble	11
4.5	Bubble growth and coalescence	14
4.6	Terminal velocity and bubble shape.....	16
4.7	Gas voidage.....	19
4.8	Conductivity and mass transfer	21
4.9	Electrode kinetics.....	22
4.9.1	Nernst and Tafel equation.....	22
4.9.2	Equations governing cell potential.....	23
4.10	Dissolving time of a small bubble.....	27
4.11	Hydrogen Transport	31
<i>Chapter 5.</i>	Experimental	33
5.1	Equipment.....	33
5.2	Procedure	35
5.3	Results and discussion.....	37
<i>Chapter 6.</i>	Conclusion	40
<i>Chapter 7.</i>	Recommendations.....	41
<i>Chapter 8.</i>	Addendum.....	42
	Risk analysis.....	42
<i>Chapter 9.</i>	References.....	45

Nomenclature

Symbol	unity	
A	m^2	surface
D	m^2/s	diffusivity
E	J	energy
F	$C/mole$	Faraday constant: 96.485 C/mole
$F_{\text{subscript}}$	N	force
I	A	current
L	m	distance from electrode gap entrance
M	$g/mole$	molar mass
P	Pa	pressure
R	$J/(mole \cdot K)$	universal gas constant: 8,31 J/(mol K)
R	Ω	resistance
S	$mole/(m^3, Pa)$	solubility
T	K	temperature
U	V	voltage
V	m^3	volume
c	$mole/m^3$	concentration
d	m	diameter
f	-	partial free area
g	m/s^2	gravitational acceleration: 9,81 m/s ²
i	A/m^2	current density
m	g	mass
r	m	radius
s	m	distance electrode gap
t	s	time
v	m/s	velocity
w	m	width of the electrode
x	m	coordinate over the width of the electrode gap
y	m	coordinate over the height in the electrode gap
z	-	# exchanged electrons
d_e	m	equivalent diameter
d_h	m	hydraulic diameter
C_d	-	drag coefficient

Eo	-	Eötvös number
Re	-	Reynolds number
\dot{n}	$mole/(m^2.s)$	molar flux
$w\%$	%	weight percent
Sh	-	Sherwood number
Sc	-	Schmidt number
k_m	m/s	mass transfer coefficient
k_b	-	Boltzmann's constant
η_{eff}	-	current efficiency
η_a	V	overpotential at the anode
η_c	V	overpotential at the cathode
f_G	-	efficiency of gas evolution
Δz	m	boundary layer thickness
α	-	charge transfer coefficient
δ	m	thickness of bubble curtain
ε	-	gas voidage or gas hold up
η	-	current efficiency
μ	$Pa.s$	dynamic viscosity
ρ	kg/m^3	density
σ	N/m	surface tension
κ	S/m	conductivity

List of Figures

FIGURE 1: THE SOLUBILITY DIAGRAM OF SODIUM CHLORATE AND CHLORIDE IN WATER FOR DIFFERENT TEMPERATURES. [14].....	5
FIGURE 2: HYDROGEN SOLUBILITY IN A SODIUM CHLORIDE AND SODIUM CHLORATE SOLUTION.	7
FIGURE 3: TWO BUBBLES WITH AN EQUAL VOLUME. THE BUBBLE IN THE CAVITY HAS A LARGER RADIUS THAN THE SPHERICAL BUBBLE.....	9
FIGURE 4: THE WETTING ANGLE INFLUENCES THE RADIUS OF BUBBLES WITH AN EQUAL VOLUME AND ADHERING AT A SURFACE.	10
FIGURE 5: THERMODYNAMICS PREDICT THAT TWO BUBBLE WILL HAVE A LOWER STATE OF ENERGY IF THEY COALESCE. AN ENERGY BARRIER MUST BE OVERCOME BEFORE COALESCENCE OCCURS.	14
FIGURE 6: AN INCREASE IN CURRENT DENSITY CORRESPONDS TO AN INCREASING VOIDAGE UNTIL THE MAXIMUM PACKING DENSITY IS REACHED. AT THIS POINT THE HOMOGENEOUS REGIME, WHICH IMPLIES THE ABSENCE OF COALESCENCE, CHANGES TO THE HETEROGENEOUS REGIME WHERE LOTS OF COALESCENCE OCCURS.	19
FIGURE 7: THE TOTAL POTENTIAL DROP CAN BE DIVIDED OVER THE POTENTIAL ON THE ANODE AND CATHODE, THE POTENTIAL DROP IN THE BULK AND THE POTENTIAL DROP IN THE BUBBLE CURTAIN.	23
FIGURE 8: THE VOIDAGE IS CONSIDERED CONSTANT IN THE BULK AND STARTS INCREASING LINEARLY DUE TO THE BUBBLE CURTAIN. THE THICKNESS OF THE BUBBLE CURTAIN IS DENOTED AS δ	25
FIGURE 9: THIS GRAPH PRESENTS THE CURRENT DENSITY WITH CORRESPONDING CELL VOLTAGE FOR A CHLORATE ELECTROLYTE UNDER INDUSTRIAL CONDITIONS. THE HIGH LIQUID VELOCITY IS 10 m/s , WALL VOIDAGE IS $0,5$. THE OTHER PARAMETERS CAN BE FOUND IN CHAPTER 4.1.	26
FIGURE 10: SMALL BUBBLES ARE FORMED CLOSE TO THE CATHODE, FURTHER AWAY FROM THE CATHODE MORE LARGER BUBBLES ARE SEEN.	28
FIGURE 11: THE EQUIPMENT USED AND DEPICTED HERE ARE AN INNER AND OUTER TUBE, SPIRAL LINKED WITH WARMWATER BATH, BASIS FIXED WITH BOLTS AND RUBBER RINGS. THE HOSES AND PH METER ENTERING THE SYSTEM FROM BELOW ARE NOT DEPICTED HERE. THE NUMBERS IN THE DRAWING ARE A LENGTH AND THEIR UNIT IS MM. [41]	33
FIGURE 12: TOP VIEW OF THE INNER VESSEL. THE POSITION OF THE PH ELECTRODE, ANODES AND CATHODES, ELECTROLYTE OUTLET AND HCL INLET ARE ALL LOCATED INSIDE THE INNER VESSEL. THE BLUE DOTS ARE THE CURRENT FEEDERS TO THE ELECTRODES.	34
FIGURE 13: THE Y-VALUES ARE THE VOIDAGES IN THE RISER TUBE IN TABLE 10 AND TABLE 11. THE X-VALUES ARE THE CURRENT. THESE RESULTS ARE FOR ONE ELECTRODE GAP WITH ELECTRODES MEASURING 3 BY 5 CM. THE 2 AND 3 LITER RESEMBLES THE TOTAL AMOUNT OF ELECTROLYTE POURED IN THE BUBBLE REACTOR.	38
FIGURE 14: THE TWO RED ARROWS SHOW AN UNUSED ELECTRODE CONNECTION AND AN ELECTRODE CONNECTION WHERE MELTING AND BURNING OCCURRED.	39
FIGURE 15: THIS DIAGRAM DIVIDES BUBBLES WITH DIFFERENT SHAPES DEPENDING ON REYNOLDS AND EÖTVÖS NUMBER BUBBLES. THE RED DOT CORRESPONDS FOR THE REYNOLDS AND EÖTVÖS NUMBER FOR A BUBBLE OF $0,1\text{ mm}$ (TABLE 5)AND CAN BE CONSIDERED SPHERICAL. [21].....	43
FIGURE 16: THIS FIGURE SHOWS THE GRAPHICAL CORRELATIONS BETWEEN REYNOLDS, NUSSELT AND PRANDTL FOR FORCED CONVECTION. [42] THESE NUSSELT AND PRANDTL NUMBERS ARE THE HEAT EQUIVALENTS OF RESPECTIVELY SHERWOOD AND SCHMIDT, WHICH ARE	

USED IN MASS TRANSFER. IN THIS GRAPH, NUSSELT AND PRANDTL MAY BE CHANGED AT ANY TIME BY SHERWOOD AND SCHMIDT. THE RED DOT CORRESPONDS FOR THE REYNOLDS NUMBER OF 4257, A LENGTH (L) OF 0.5 M AND D OF 3 MM. 44

List of Tables

TABLE 1: THE TOTAL AMOUNT OF MOLE IN A TYPICAL SOLUTION UNDER INDUSTRIAL CONDITIONS IS CALCULATED. E STANDS FOR ELECTROLYTE.	7
TABLE 2: MAXIMUM SOLUBILITY OF HYDROGEN IN A 8% CHLORIDE AND 43% CHLORATE SOLUTION.	7
TABLE 3: DIFFERENT BUBBLE DIAMETERS AND THEIR INTERNAL PRESSURE WITH CORRESPONDING MAXIMUM CONCENTRATION FOR TWO DIFFERENT DEPTHS.	8
TABLE 4: THE EFFICIENCY OF GAS EVOLUTION INCREASES WITH INCREASING CURRENT DENSITY FOR A PLATINA ELECTRODE AND STIRRED ELECTROLYTE [13]	11
TABLE 5: REYNOLDS AND EÖTVÖS NUMBERS FOR DIFFERENT EQUIVALENT DIAMETERS AND A TERMINAL VELOCITY OF 0,001 m/s ARE TABULATED.	17
TABLE 6: THE EXTRA VELOCITY DUE TO THE SWARM CHANGES WITH DIFFERENT VOIDAGES. THE VALUE OF THE VELOCITY OF A SINGLE BUBBLE IS THE ONE THAT IS CALCULATED EARLIER THIS CHAPTER.	18
TABLE 7: THE POTENTIAL DROP BETWEEN TWO ELECTRODES FOR CURRENT DENSITY OF 2000 A/m ² . THE BRUGGEMAN EQUATION PREDICTS HIGHER POTENTIAL DROPS FOR HIGHER VOIDAGES DUE TO LOWER ELECTROLYTE RESISTANCE.	21
TABLE 8: THE DISSOLVING TIME AND SPEED FOR SEVERAL BUBBLE SIZES IN THE VICINITY OF A 0.1 MM BUBBLE.	29
TABLE 9: THE VOLUME OF A BUBBLE WITH THE REQUIRED DISSOLVING VOLUME FOR DIFFERENT BUBBLE SIZES. ALSO THE FACTOR DIFFERENCE BETWEEN THESE TWO VOLUMES IS GIVEN.	30
TABLE 10: THE RESULTS OF AN ELECTROLYSIS WITH A 2 LITER SOLUTION OF 500g/L NaClO ₃ , 100 g/L NaCl, 1.5g/L NaOH AND 5g/L Na ₂ Cr ₂ O ₇ . TWO ELECTRODES ARE USED.	37
TABLE 11: THE RESULTS OF AN ELECTROLYSIS WITH A 3 LITER SOLUTION OF 500g/L NaClO ₃ , 100 g/L NaCl, 1.5g/L NaOH AND 5g/L Na ₂ Cr ₂ O ₇ . TWO ELECTRODES ARE USED.	37

Chapter 1. Introduction

Eka Chemicals is a daughter company of AkzoNobel and one of their main products is sodium chlorate (NaClO_3). It is used in the pulp and paper industry for the production of chlorine dioxide which is an important bleaching chemical. Chlorate is used as a chemical oxygen generator in airplanes where it provides emergency oxygen in case of pressure drop. Potassium chlorate in matches is also made from sodium chlorate. Chlorate is used as a total destructive herbicide in the agricultures sector and as raw material for the production of perchlorates and perchloric acid.

Chlorate is produced electrochemically. When current is sent through an electrolyte of salt in water, hydrogen gas is formed at the cathode as a byproduct. This gas drives the convection in the cell due to the buoyancy caused by the gas bubbles. Gas evolution also has some undesirable effects such as reducing the conductivity. The effect of a change in conductivity on the mass transfer is still to be discussed.

Electrolysis is a power consuming process. Assuming 100 % current efficiency, the chlorate process needs a charge of 1,51 MAh for the production of one ton of chlorate. This is calculated with Faraday's Law (Eq.(1.1)). To run an electrolyzer, a superimposed potential around 3 V is needed. The precise cell voltage depends on the cell design and operating conditions such as current density, flow rate and temperature. The current efficiency (η_{eff}) of the sodium chlorate process ranges between 93 and 96%. [27]

$$It = \frac{mzF}{M} \quad (1.1)$$

The total power consumption is given by the equation below: [27]

$$\text{Power consumption} = \frac{I \cdot t \cdot U}{\eta_{eff}} = \frac{1,51 \cdot 10^6 \text{ A} \cdot 1 \text{ h} \cdot 3 \text{ V}}{0,95} = 4,8 \text{ MWh} \quad (1.2)$$

This makes a power consumption of 4,8 MWh per ton chlorate. When taking in account the price of one MWh and the annual production of chlorate, the electricity costs at Eka Chemicals is 200-300 million Euro every year. Even the smallest improvements on current efficiency or on the total voltage would lead to large savings.

The chlorate process is greatly dependent on mass transfer and transport of reacting species to and from the electrode surfaces. Since hydrogen bubbles have an effect on the mass transfer and conductivity, their behaviour has to be examined. Also other information like bubble size, bubble growth and hydrogen transport will be searched for to create a better understanding of hydrogen bubbles. After all, these bubbles causes a higher cell voltages and therefore a higher power consumption. The reason why a better bubble understanding is searched for is to reduce the costs of the cell voltage caused by these bubbles by bubble coverage on the electrode, gas voidage and bubble curtain.

Chapter 2. Chlorate cell

There are multiple reactions occurring in the chlorate cell. They can be split up in wanted and parasitic reactions. The overall reaction is formulated by equation (2.1). [25]



2.1 Wanted reactions

The following reactions are the wanted reactions that take place at the anode. Chloride is oxidized to chlorine and after a few more reactions chlorate is formed. Equations (2.3) and (2.5) are disproportionation reactions.



Reaction (2.5) has the highest reaction rate when the ratio $[HClO]/[ClO^-]$ is equal to 2, thus

$$pH = pK_a - \log(2) \quad (2.6)$$

The reduction of water is the wanted reaction at the cathode. The electrons pass from the anode through a direct current power supply to the cathode.



2.2 Parasitic reactions

The anodic oxygen formation is an unwanted side reaction which consumes 4 to 6% of the imposed current and thereby lowers the current efficiency. Oxygen is mainly produced by the electrochemically oxidation of water and the decomposition of hypochlorous acid. [2] Lowering the oxygen formation is a very important topic in optimizing the chlorate cell, but it will not be of further discussion in this work.

The cathodic reduction of hypochlorite and chlorate are the most important side reactions. They are inhibited by the addition of sodium dichromate. After some reactions sodium dichromate forms a chromium hydroxide layer on the cathode. [33] The sodium dichromate also acts as a buffer, which helps keeping the cell at the desired pH .

Chapter 3. **Goal**

In chlorate electrolysis hydrogen bubbles are formed at the cathode. These bubbles lower the conductivity of the electrolyte which results in a higher electrical potential leading to higher power consumption.

In order to find a way to reduce the electricity costs, it is important to understand how the bubbles are formed and how they behave.

The objectives of this study are:

1. To setup an experimental method to measure the maximum packing density of the hydrogen bubbles as a function of independent variables like temperature and concentrations.
2. To determine the maximum packing density of the hydrogen bubbles and the current density at which this limiting voidage is reached under industrial conditions.
3. To determine an equation for the dissolving time of small bubbles and an equation for the minimum possible bubble size at the cathode.
4. To develop equations for the potential over the electrode gap depending on different parameters to find out the effect of these parameters on the potential.

The aim of this present work is to provide information to be used in CFD modeling of the electrode gap. Both the findings about the packing density and the developed equations will help to give a better understanding of how bubbles behave.

Chapter 4. Two-phase flow in an electrode gap

4.1 Chlorate electrolyte

Before going deeper into detail in the chlorate process, some values of parameters that will be used, are written here. For some of them also a brief explanation is added to see how they are calculated.

The typical composition of the chlorate electrolyte and its physical properties are tabulated below. Unless differently mentioned, these values will be used in further calculations. The mass percentages of 8% and 43% of chloride and chlorate are numbers representative under industrial conditions. Same line of reasoning accounts for the temperature of 70°C , the inter-electrode distance of 3 mm and an electrode length of $0,5\text{ m}$.

mass percentage NaCl	8%
mass percentage NaClO_3	43%
density electrolyte [19]	1419 kg/m^3
density hydrogen bubble	1 kg/m^3
bubble diameter[1]	$0,0001\text{ m}$
temperature	70°C
conductivity [23]	$37,8\text{ S/m}$
vapor pressure of water [19]	180 mmHg
hydrogen solubility [20]:	$0,3 \cdot 10^{-5}\text{ mole fraction}$
surface tension [44]	$0,0644\text{ N/m}$
electrode gap	$0,003\text{ m}$
terminal velocity bubble	$0,0068\text{ m/s}$
liquid velocity [25]	$0,5\text{ m/s}$
viscosity continue phase [1]	$0,001\text{ kg/(m.s)}$
thickness bubble layer [1]	$0,0005\text{ m}$
wall voidage	0,5
diffusivity[17]	$6,73 \cdot 10^{-9}\text{ m}^2/\text{s}$
electrode length	$0,5\text{ m}$

In later calculations all bubbles are considered to have a diameter of $0,1\text{ mm}$ since this is a common size of hydrogen bubbles in the electrode gap in the chlorate process when no coalescence occurs [1]. A typical composition of the electrolyte under industrial conditions is 8% NaCl and 43% NaClO_3 . The electrolyte also contains 3-7 g/L $\text{Na}_2\text{Cr}_2\text{O}_7$. The density of this mixture is 1419 kg/m^3 at 70°C . [19] Liquid velocity is chosen as $0,5\text{ m/s}$ [25]. The terminal velocity of a single 1 mm bubble is calculated in chapter 4.6.

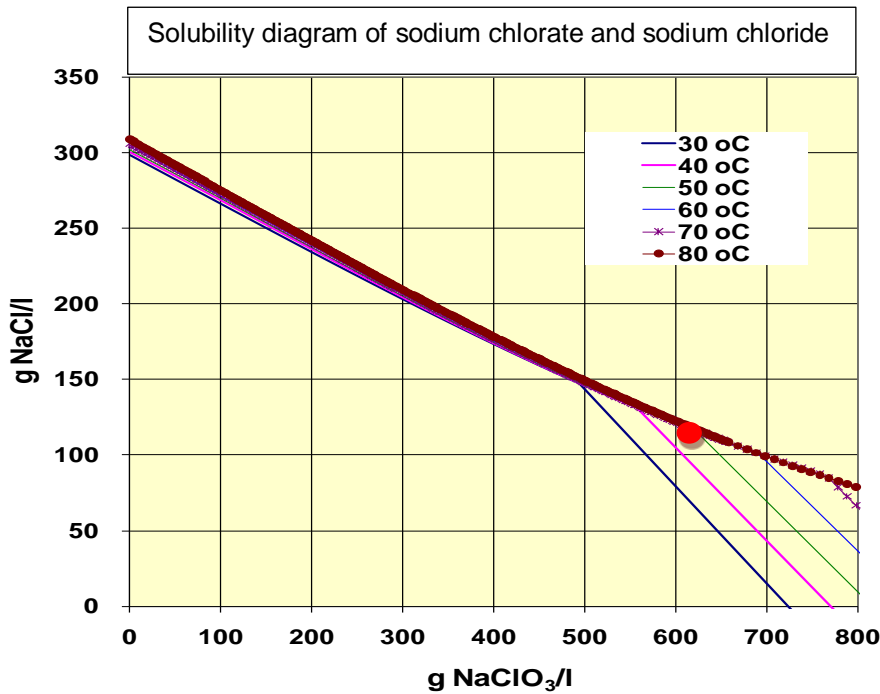


Figure 1: The solubility diagram of sodium chlorate and chloride in water for different temperatures. [14]

The graph in Figure 1 shows the phase diagram for $NaCl$ and $NaClO_3$ dissolved in water. It explains the concentration levels in the cells. More chlorate is soluble when the temperature is increased. The red dot indicates the point of 115 g $NaCl$ and 610 g $NaClO_3$ (8% and 43% of the density). A saturated brine solution gives a maximum current efficiency and a minimal cell voltage. [27]

The diffusion coefficient is found out of the Stokes-Einstein equation. Out of this equation another equation can be found that predicts the dependence of the diffusion coefficient for different temperatures and viscosities.[17] The values of diffusivity and viscosity of a electrolyte consisting of 8% $NaCl$ and 43% $NaClO_3$ with a temperature of 70°C are given the index 1. The values of diffusivity and viscosity for pure water under standard conditions are denoted with index 2.

$$\frac{D_1 \mu_1}{T_1} = \frac{D_2 \mu_2}{T_2} \quad (4.1)$$

$$D_1 = \frac{T_1 \mu_2}{T_2 \mu_1} D_2 = \frac{343 \cdot 0,001}{298 \cdot 0,001} 5,85 \cdot 10^{-9} = 6,73 \cdot 10^{-9} m^2/s \quad (4.2)$$

After implementing the values for new viscosity and temperature the diffusivity of hydrogen under industrial conditions is found.[1][17]

4.2 Hydrogen formation and superficial gas velocity

In the chlorate process hydrogen is formed at the cathode by the following reduction:



It takes two moles of electrons for the formation of one mole of hydrogen. Equation (4.4) shows the molar flux of hydrogen. When the current is increased, more electrons will be available and more hydrogen will be formed. The molar rate of production is given by:

$$\dot{n}_{H_2} = \frac{i}{2F} \quad (4.4)$$

The produced hydrogen will form bubbles. The buoyancy of the bubbles is responsible for the convection in the electrode gap. Increasing the current will enhance the hydrogen formation. More bubbles leads to a higher velocity of the gas-liquid dispersion due to higher lift forces. A commonly used way for describing the hydrogen formation is the superficial gas velocity (v_g). It describes the volumetric gas flow formed on an electrode area or passing a certain cross section area (Eq.(4.5)). [8] At the entrance of an electrode gap the superficial gas velocity will be very low. It will not be zero because there might be small bubbles in the circulating electrolyte. The superficial gas velocity will increase when moving upwards in the electrode. It will also increase with an increasing current density.

$$v_g = \frac{I}{2F} \cdot \frac{RT}{P_T - P_{water}} \cdot \frac{1}{A_{electrode}} \quad (4.5)$$

Besides hydrogen, bubbles also contain water. Only the hydrogen pressure may be used to calculate the superficial velocity of hydrogen (Eq.(4.6)). In Equation (4.7), the water pressure (P_{water}) is linked to the temperature and the mass percent of chlorate.[19] A temperature of 70°C and 51 w% gives a water vapor pressure in chlorate of 180 mmHg.

$$P_{H_2} = P_{Total} - P_{water} \quad (4.6)$$

$$P_{water} = \frac{180}{760} \quad (4.7)$$

Hydrogen is formed as a dissolved gas. Only above a certain concentration it will start to form bubbles. This saturation concentration depends on the roughness and material of the cathode and on the hydrostatic pressure.

Depending on the concentration of the chloride and chlorate, a different amount of hydrogen is soluble in the electrolyte. As seen in Figure 2 below, for a solution of about 115 and 610 gram/liter of respectively $NaCl$ and $NaClO_3$ the solubility concentrations is $0,3 \cdot 10^{-5}$ mole H_2 /mole electrolyte. [20] This solution has chlorate and chloride combined. The red dot on Figure 2 combines 7,67 mole (which is the sum of 1,94 mole chloride and 5,73 mole chlorate as can be seen in Table 1) in one liter electrolyte and the temperature of 70°C.

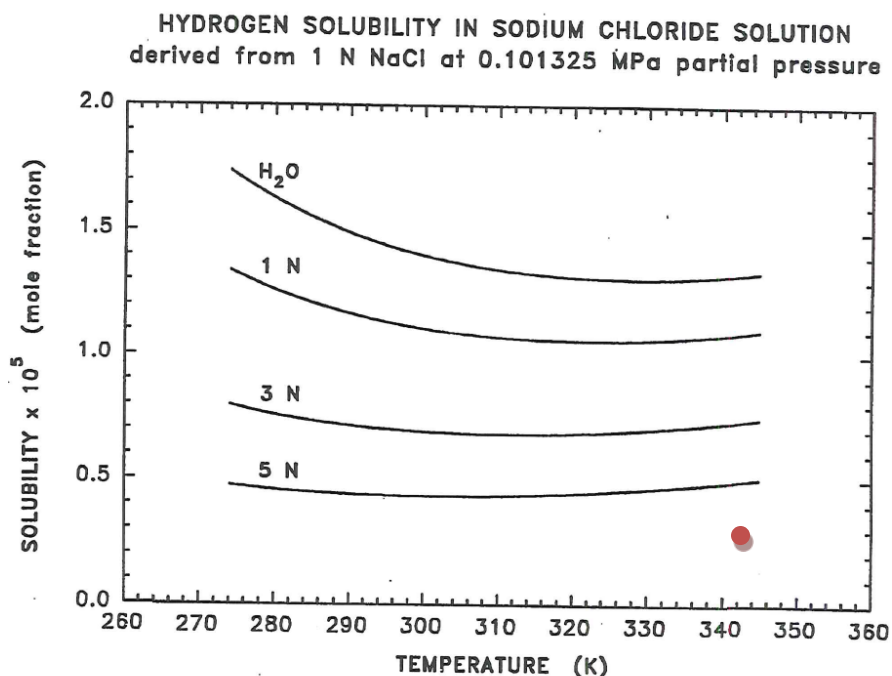


Figure 2: Hydrogen solubility in a sodium chloride and sodium chlorate solution.

The reason why this solubility constant is calculated, is to link the pressure inside a bubble with the saturation concentration around that bubble. This solubility constant will be used with the calculation for the minimum bubble size at the cathode in chapter 4.4.

Table 1: Solubilities at 1 bar H₂. The total amount of mole in a typical solution under industrial conditions is calculated. E stands for electrolyte.

	w%	M (g/mole)	mole /L E
NaCl	8	58,5	1,94
NaClO ₃	43	106,5	5,73
H ₂ O	49	18	38,63
Total			46,3

Table 2: Maximum hydrogen solubility at 1 bar H₂ in a 8% chloride and 43% chlorate solution .

	Mole E/L E	S (mole H ₂ /L E)	S (mole H ₂ /m ³ E)
Total	46,3	0,00014	0,14

$$S = 46,3 \frac{\text{mole } E}{\text{Liter } E} \cdot 0,3 \cdot 10^{-5} \frac{\text{mole } H_2}{\text{mole } E, \text{bar}} = 0,00014 \frac{\text{mole } H_2}{\text{Liter } E, \text{bar}} \quad (4.8)$$

$$S = 0,14 \frac{\text{mole}}{\text{m}^3, \text{bar } H_2} = 0,14 \cdot 10^{-5} \frac{\text{mole}}{\text{m}^3, \text{Pa } H_2} \quad (4.9)$$

The maximum solubility (S) of hydrogen in the electrolyte is obviously about 0,14 mole/m³,bar H₂. Above this concentration hydrogen bubbles might be formed depending on bubble size, nucleation sites and hydrostatic pressure.

4.3 Bubble formation

A hydrogen bubble can only be formed if the hydrostatic pressure is lower than the saturation pressure of hydrogen and water. Supersaturation can be seen as the driving force for nucleation. Equation (4.10) is derived from the Young-Laplace equation.[34] It relates the pressure drop across the interface with the curvature of the surface, represented as the diameter here.

$$(P_{\text{inside}} - P_{\text{outside}}) = (P_{H_2} + P_{H_2O} - P_{\text{outside}}) = \frac{4\sigma}{d} \quad (4.10)$$

$$P_{\text{outside}} = \rho \cdot g \cdot h + P_{\text{atm}} \quad (4.11)$$

The hydrostatic pressure is P_{outside} . The internal pressure of a bubble will often be referred to as the Laplace pressure. Different saturation pressures, found in Table 3, depend on the bubble size and the depth in the electrolyte. Compared with bubble size, the depth only has little influence on the saturation concentration, especially for smaller bubbles.

Table 3: Different bubble diameters and their internal pressure with corresponding maximum concentration for two different depths.

h (meter)	d (meter)	P _{H2} (bar)	c _{sat} (mol H ₂ /m ³)
0,5	1,00E-04	0,87	0,12
0,5	1,00E-05	1,11	0,15
0,5	1,00E-06	3,50	0,49
0,5	1,00E-07	27,41	3,81
0,5	1,00E-08	266,45	37,01
0,05	1,00E-04	0,81	0,11
0,05	1,00E-05	1,05	0,15
0,05	1,00E-06	3,44	0,48
0,05	1,00E-07	27,34	3,80
0,05	1,00E-08	266,4	37,00

Equation (4.12) explains how the last column of Table 3 is calculated. The maximum solubility S is calculated before in Table 2.

$$P_{H_2} \cdot S = c_{saturation} \quad (4.12)$$

$$[bar] \left[\frac{mol H_2}{m^3 E, bar H_2} \right] = \left[\frac{mol H_2}{m^3} \right] \quad (4.13)$$

Table 3 shows that both high saturation pressures and high hydrogen concentrations are needed to generate bubbles of micrometer size or smaller. The difference in hydrostatic pressure only gives a small difference of the internal pressure of the bubble. The last column shows the required saturation pressure of hydrogen in the liquid. A bubble will continue to grow until its internal pressure equals the saturation pressure. When a full grown bubble moves away from the electrode to places with lower hydrogen concentration its internal pressure will become too high and the bubble will get smaller by diffusion or absorption of hydrogen back into the electrolyte until equilibrium by the Young-Laplace equation is found.

If the electrolyte is saturated with hydrogen near the cathode, bubble formation will start at nucleation points at the electrode surface. [43] This process is called heterogeneous nucleation. It can be considered as a surface catalysed or assisted nucleation surface. Homogeneous nucleation occurs only inside the bulk without a surface near and it requires a higher concentration of hydrogen.

The nucleation point is an irregularity; generally a cavity on the cathode surface. Already existing bubbles can also act as a surface. The smaller the radius of a bubble, the higher the pressure inside must be. For this reason bubble formation will occur in cavities. The radius here will be much larger than it would be at a flat surface (see Figure 3). The moment a bubble detaches from the cavity into the bulk, the radius decreases and the internal pressure increases a lot.

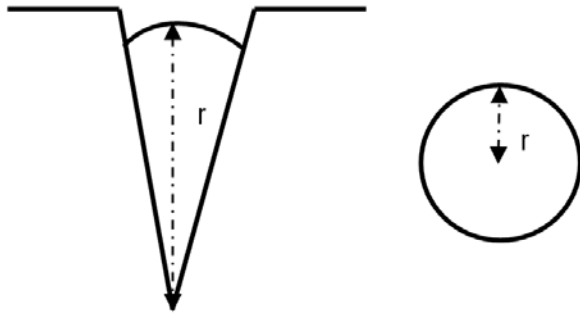


Figure 3: Two bubbles with an equal volume. The bubble in the cavity has a larger radius than the spherical bubble.

Figure 3 shows two bubbles with the same volume. The one still attached to the nucleation point has a larger radius and therefore also a lower internal pressure and can therefore be formed with lower saturation concentrations.

Another property that will influence the nucleation is the wetting angle θ (Figure 4). It is determined by the resultant between adhesive and cohesive forces. A higher wetting angle gives larger radius of the bubble.

The wetting angle is the angle at which the liquid–vapor interface meets the solid–liquid interface. A surface promotes nucleation because of wetting. Contact angles greater than zero between phases facilitate particles to nucleate. The free energy needed for heterogeneous nucleation is equal to the product of homogeneous nucleation and a function of the contact angle [31]. The subscripts in the equation below refers to heterogeneous and homogeneous nucleation.

$$\Delta G_{heterogeneous} = \Delta G_{homogeneous} \cdot f(\theta) \quad (4.14)$$

$$f(\theta) = \frac{2 - 3 \cos \theta + \cos^3 \theta}{4} \quad (4.15)$$

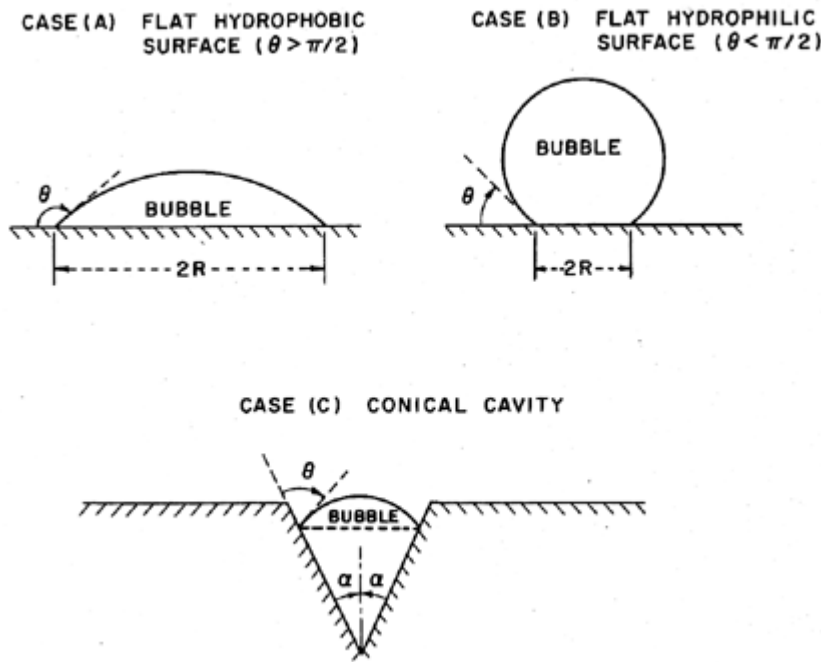


Figure 4: The wetting angle influences the radius of bubbles with an equal volume and adhering at a surface.

A higher wetting angle goes along with a higher radius of the bubble and therefore a lower internal pressure which in turn means that bubbles can be formed at lower hydrogen concentrations. [32]

Surface tension is the measure of the intermolecular forces that tend to hold molecules together. Larger surface tension equals larger cohesive forces which results in a lower wetting angle. It is important to remember that both the roughness and the type of electrode will influence the nucleation. Deeper cavities and higher wetting angles favors nucleation since they both give rise to a larger radius for the same amount of hydrogen available.

There are different mechanisms that transport away the hydrogen formed at the electrode [13]. Depending on the current density they take place both at the same time or just one of them occurs. The first mechanism is convective mass transfer to the bulk. Another one is transfer from the region near the electrode to the gas-liquid interface of growing bubbles adhering to the electrode, subsequent

transformation into the gaseous phase and bubble departure from the electrode. If the current density is very low, there will only be convective mass transfer and no bubble formation because the saturation point of hydrogen will not be reached.

The efficiency of gas evolution (f_G) is defined as the fraction of hydrogen transported away from the electrode in the form of bubbles. At low current densities f_G is zero, which means convective mass transfer is the only way of transporting the produced hydrogen away from the electrode. [8] At some point f_G starts increasing proportionally with the current density until there is maximum efficiency of gas evolution. [13] Below 10 A/m^2 no gas evolution occurs although there might be regions with higher concentration which will activate nucleation points resulting in local bubble formation. A few values of the efficiency of gas evolution can be found in Table 4. [13]

Table 4: The efficiency of gas evolution increases with increasing current density for a platina electrode and stirred electrolyte [13]

$i \text{ (A/m}^2\text{)}$	f_G
1000	0,07
2000	0,2
10 000	0,4

4.4 Concentration boundary layer and minimum bubble

The smallest possible bubble at the cathode and the boundary layer thickness are calculated here. Both the boundary layer thickness as the smallest bubble size will be compared with the average size in the bulk.

The Laplace pressure of the average size bubble gives information about the partial pressure of hydrogen in the bubble (see Eq.(4.10)) and the corresponding bulk concentration of hydrogen. The smallest possible bubble in the cell exists where the hydrogen partial pressure and the concentration of dissolved hydrogen are at maximum i.e. at the cathode wall.

The concentration difference over the boundary layer is calculated with the use of mass transfer coefficient k_m (Eq.(4.16)) which relates the mass flux with the difference in concentration, which is the driving force of the mass transfer. Efficiency of gas evolution (see Table 4) is added in the molar flux in equation (4.4) to get equation (4.17).

$$\dot{n}_{H_2} = k_m \Delta c = k_m (c_{H_2, cathode} - c_{H_2, bulk}) \quad (4.16)$$

$$\dot{n}_{H_2} = \frac{i}{2F} (1 - f_G) \quad (4.17)$$

The two equations above can be rearranged to the concentration at the cathode.

$$c_{H_2, cathode} = \frac{i(1-f_G)}{2Fk_m} + c_{H_2, bulk} \quad (4.18)$$

The current density is taken as 2000 A/m^2 . The Sherwood number (Sh) is used to find the mass transfer coefficient. It can be expressed as a function of the Schmidt number (Sc) and Reynolds number (Re_h) as in Equation (4.20) [40].

$$Sh = \frac{k_m s}{D} = \frac{s}{\Delta z} \quad (4.19)$$

$$Sh = A Re^B Sc^C \quad (4.20)$$

Once this Sherwood number is found, both the boundary layer thickness and the mass transfer coefficient can be found. The constants A, B and C depend on the flow that could either be laminar or turbulent. The relative importance of the Reynolds number value in calculating the Sherwood number increases when the flow switches from laminar to turbulent.

The Reynolds number for the flow between parallel plates is calculated to find out the flow type (Eq.(4.21)). The hydraulic diameter (d_h) is twice the width of the electrode gap. The values for viscosity, density and liquid velocity can be found in chapter 4.1.

$$Re_h = \rho d_h \frac{v_{liquid}}{\mu} = 4257 \quad (4.21)$$

For this Reynolds number Equation (4.22) can be found in the diagram in Figure 16 which can be found in the addendum. [42]

$$Sh \cdot Sc^{-1/3} = 17 \quad (4.22)$$

This value accounts for a $0,003 \text{ m}$ wide and $0,5 \text{ m}$ long electrode gap. The Schmidt number in Equation (4.23) is calculated with values for viscosity, density and diffusivity coefficient found in chapter 4.1.

$$Sc = \frac{\mu}{\rho D} = \frac{0,001}{1419 \cdot 6,73 \cdot 10^{-9}} = 105 \quad (4.23)$$

Combining Equation (4.22) and Equation (4.23) gives:

$$Sh = 17 \cdot 105^{1/3} = 80 \quad (4.24)$$

Rearranging Equation (4.19) gives the equations below.

$$\Delta z = \frac{d_h}{Sh} = \frac{0,006}{80} = 7,5 \cdot 10^{-5} \text{ m} \quad (4.25)$$

$$k_m = \frac{Sh D}{d_h} = \frac{80 \cdot 6,73 \cdot 10^{-9}}{0,006} = 9,0 \cdot 10^{-5} \frac{\text{m}}{\text{s}} \quad (4.26)$$

The thickness of the boundary layer ($\Delta z = 7,5 \cdot 10^{-5} \text{ m}$) is two orders of magnitude smaller than the distance between the two electrodes ($s = 3 \cdot 10^{-3} \text{ m}$) It is of the same order of magnitude than a typical bubble diameter in the bulk which is $0,1 \text{ mm}$.

If an average bubble diameter in the bulk is known, it is possible to recalculate this diameter to an internal pressure which can in turn be recalculated to a saturation concentration. This saturation concentration will

then be used as $c_{H_2,bulk}$. The average bubble diameter in the bulk is found in Bollens' thesis [1]. For an electrolyte of 100 and 500 g/L of $NaCl$ and $NaClO_3$ at $70^\circ C$ the average bubble size halfway the length of the electrode is 0,1 mm. In Table 3 it is found that a 0,1 mm bubble corresponds to a concentration of dissolved hydrogen of $0,12 \text{ mole}/m^3$. If no bubbles are formed at the cathode surface ($f_G = 0$) Equation (4.18) will give the following result.

$$c_{H_2,cathode} = \frac{2000(1-0)}{2 \cdot 96485 \cdot 9,0 \cdot 10^{-5}} + 0,12 = 115 \text{ mole}/m^3 \quad (4.27)$$

Since this is the highest possible hydrogen concentration at the cathode, the diameter of the smallest possible bubble and its internal pressure can be calculated below. Equation (4.28) is made by combining equations (4.6) and (4.12). Equation (4.29) is nothing but the rearrangement of equation (4.10).

$$P_{in} = \frac{c_{H_2,cathode}}{s} + P_{water} = \frac{115 \text{ mole}/m^3}{0,14 \text{ mole}/(m^3, bar H_2)} + 0,25 \text{ bar} = 824 \text{ bar} \quad (4.28)$$

$$d = \frac{4\sigma}{(P_{inside} - P_{outside})} = 3,2 \cdot 10^{-9} m \quad (4.29)$$

The concentration at the cathode can be lowered by making the cathode surface rougher. In reality bubbles are formed at the surface which makes the transport of dissolved hydrogen far less and this leads to a lower surface concentration of hydrogen. In addition, the bubbles may accelerate the mass transport i.e. increase k_m which also lowers the surface concentration.

If 90% of the bubbles are formed at the surface ($f_G = 0,9$) equation (4.27) will give a lower concentration at the cathode and the theoretical minimum distance will become about $3,2 \cdot 10^{-8} m$. In Table 4 an efficiency of gas evolution of 0,2 can be found for a current density of $2000 \text{ A}/m^2$. The theoretical minimum bubble diameter then becomes $4,02 \cdot 10^{-9} m$. Higher values of f_G correspond with larger minimum bubble diameters. This is obvious since a higher amount of bubbles formed will result in a lower surrounding concentration of hydrogen which in turn results in a larger minimum bubble diameter.

The disadvantage of these small bubbles is that extra energy is needed to create bubbles with such a high Laplace pressure. The Nernst equation is used here to find the extra energy needed to form these small bubbles.

$$\Delta U = \frac{RT \ln(P/P_0)}{zF} = \frac{8,31 \cdot 343 \cdot \ln(824/1)}{2 \cdot 96485} \cong 0,10 \text{ V} \quad (4.30)$$

4.5 Bubble growth and coalescence

In the chlorate process hydrogen bubbles are formed. Whether these bubbles coalesce or not has great influence on the system. It is therefore important to have a better understanding of what coalescence is and how it can be inhibited. If two bubbles collide and coalescence occurs, the surface area of the new bubble will be smaller than that of the two small bubbles together. The change of surface energy due to coalescence is given as

$$\Delta E = \sigma_{gas-liquid} \Delta A \quad (4.31)$$

Since the surface area of the newly formed bubble will be smaller than before, the energy change will always be negative. The process of two coalescing bubbles will result in a lower state of energy. This means that seen from hydrodynamic perspective, coalescence is expected to happen (see Figure 5). However, coalescence in electrolyte solutions is not a spontaneous process as the negative change of surface energy indicates. It has been shown that coalescence does not always occur in the electrode gap of the chlorate cell.[1] Therefore, there must be an activation energy barrier for the coalescence (see Figure 5) [8].

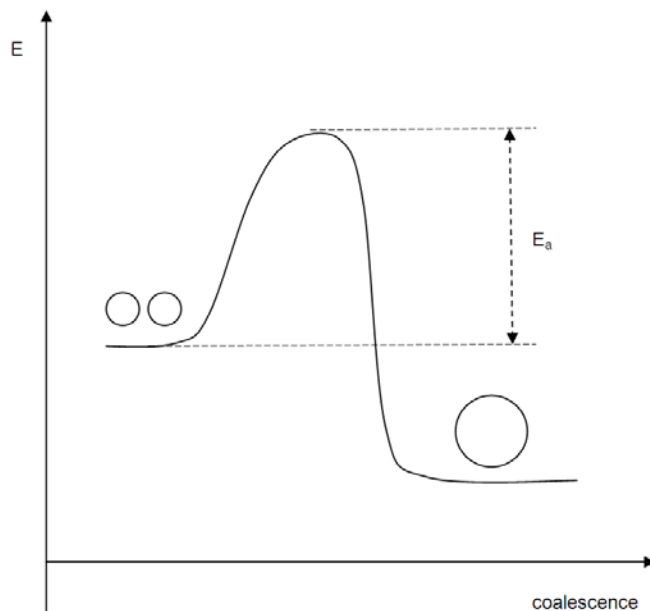


Figure 5: Thermodynamics predict that two bubble will have a lower state of energy if they coalesce. An energy barrier must be overcome before coalescence occurs.

Before going deeper into reasons that might explain this unexpected behaviour, a short description of coalescence is given. The process of coalescence can be divided in three consecutive steps [10]:

- 1) The first step is two bubbles that will approach each other which will result in the formation of a thin liquid film between liquid and gas interfaces.

- 2) The next step is the drainage of this film driven by two types of forces. The first group are the external forces (gravity, inertia of flow) that are proportional to volume of the bubble. The second group of forces that influences the drainage of the film are the surface forces of molecular origin, which are proportional to the thin liquid film area.
- 3) The last step is the film rupture which occurs at a critical thickness of the thin liquid layer h_{rupt} . Capillary and molecular forces on both sides of the liquid film will make it to become thinner until h_{rupt} is reached which will lead to the bubble coalescence.

The first step, the bubble approach, is heavily influenced by the gas flow rate. An increased gas flow rate produces a higher amount of bubbles per unit volume and thereby, the frequency of collision rises too. Another reason how it enhances coalescence is because a higher flow rate generates stronger convection which implies a more effective impact of the bubbles. [5] [10]

There are two possible reasons that might explain the activation barrier that must be overcome for coalescence to take place. The first one is an increased liquid pressure close to the gas liquid interface that leads to certain repulsion when two bubbles approach each other. Liquid molecules get attracted due to their asymmetric surrounding which results in this small layer of increased pressure around the bubble.[8] The second reason that might explain this activation barrier is that gas bubbles in electrolyte solution have an excess of OH^- near the gas liquid interface which causes a negative surface charge. This will in turn give an electrostatic repulsion that again retards the coalescence process.[38]

If bubbles get more closely packed, the distance between two bubbles will decrease. When the limiting voidage is reached, the bubbles are in the maximum packing density. The bubbles are now separated by a certain minimum distance from each other without coalescence will occur. Whenever bubbles will cross this minimum distance, coalescence will take place which makes that the voidage will increase no more. The limiting voidage depends on both the bubble diameter and the minimum distance between two bubbles. The lattice type of the bubbles in the bubble curtain will predict the minimum bubble distance.[8]

Addition of salt ions to the two-phase flow will affect the coalescence behaviour of the bubbles [10]. The concentration of the salt at which half of the bubble collisions will result in coalescence is called the transition concentration c_{trans} . The value c_{trans} depends on the type (size and polarizability) of the ions and their combination. [10] Tsang et al. reported the first evidence of c_{trans} dependence on bubble size.[11] Gas velocity is more important than size of the bubble. Greater electrolyte concentrations also give rise to smaller bubbles. [5]

Not all ion types inhibit coalescence. Craig has demonstrated that some combinations of ion pair do inhibit coalescence while others don't [39]. A combination pair of two hard and small or two soft and large ions will inhibit coalescence and the combination of a soft and hard ion will not inhibit coalescence.

To have a better understanding of what ions do and don't inhibit coalescence, Collins's concept of matching water affinities should be known. The interpretation of this concept is that oppositely charged ions will form direct ion pairs spontaneously if they have equal water affinities. Two small and hard ions of opposite charge will be strongly hydrated and are capable of attracting one another in order to form a direct ion pair. The hydration layers between them are repelled in the process. Two large and soft ions of opposite charge will be weakly hydrated and will also form a direct ion pair when they approach. Their electrostatic attraction is much smaller compared to the two small and hard ions, but their hydration layer is more loosely bound. In the case of a combination a small strongly hydrated and a large ion with loose hydration layer there will always be a surrounding water shell preventing them to form an ion pair. Whether or not the two ions of opposite charge are capable of forming a direct ion pair has an influence on the coalescence inhibition.[10]

4.6 Terminal velocity and bubble shape

The bubble shape is determined in this chapter. This is necessary for the calculation for the terminal velocity afterwards. The terminal velocity of a gas bubble will be compared with the liquid velocity to see if volumes can be changed by velocities for the calculations of the voidages (see chapter 4.7). The gas voidage will then be used for the calculations of the conductivity which will in turn be used in the equations for the potential in the electrode gap.

The buoyancy is the upward force that a fluid exerts on an object less dense than itself. When these buoyancy effects are taken into account, an object falling through a fluid under its own weight can reach a terminal velocity if the net force acting on the object becomes zero. When the terminal velocity is reached, the weight of the object is exactly balanced by the upward buoyancy force and drag force. The line of reasoning is the same for a gas bubble rising in a liquid. In reality the different forces acting on a bubble never balances each other, so the motion of the bubble always remains unsteady. Therefore, the terminal velocity of a bubble is best to be understood as a time averaged rise velocity of a bubble. [18][21]

Not every bubble is spherical shaped. Bubbles can be deformed due to external fluid fields until normal and shear stresses are balanced at the fluid-fluid interface. It is possible for rising bubbles in infinite media to prepare a graphical correlation in terms of Eötvös number and the Reynolds number (Figure 15). Both of them are dimensionless numbers. Reynolds number (Eq.(4.32)) is a ratio of inertial forces to viscous forces while the Eötvös number (Eq.(4.33)) is the ratio of buoyancy to surface tension. [21] In Table 5 some values for Re and Eo can be found for a terminal velocity of $0,001\text{ m/s}$.

$$Re = \rho d_e \frac{v_L}{\mu} \quad (4.32)$$

$$Eo = g \Delta \rho \frac{d_e^2}{\sigma} \quad (4.33)$$

Table 5: Reynolds and Eötvös numbers for different equivalent diameters and a terminal velocity of **0,001 m/s** are tabulated.

d_e (m)	Re	Eo
0,01	14,19	21,60
0,001	1,419	0,216
0,0001	0,1419	0,002

Bubbles of 0,1 mm in diameter are representative in the electrode gap [1]. In the graph in Figure 15 found in the addendum, it can be seen that bubbles with this diameter have Reynolds and Eötvös numbers characteristic for a spherical bubble. It is commonly observed that small bubbles do obey Stokes law and have no internal circulation [21]. It must be said that a bubble is termed as spherical if the minor to major axis ratio lies within 10% of unity. For other calculations made below, the bubble will be considered fully spherical if it is determined spherical in the graph presented in Figure 15.

The buoyancy is the weight of the displaced liquid. After calculating the Eötvös and Reynolds number it can be concluded that the bubble is a sphere. Therefore it is allowed to use the volume of a sphere in the formula of the buoyancy. At terminal velocity drag and buoyancy forces are equal. [28]

$$F_{buoyancy} = \frac{4}{3} r^3 \pi \rho g \quad (4.34)$$

$$F_{drag} = C_d \pi r^2 \rho \frac{v_d^2}{2} \quad (4.35)$$

For the formula of drag coefficient (C_d) Equation (4.36) is used which is only applicable for Re numbers below 800. As calculated before, Re is very low and the well-known Schiller-Naumann equation can be used:[21]

$$C_d = \frac{24}{Re} (1 + 0,15 Re^{0,687}) \quad (4.36)$$

In an Excel sheet, the Excel solver is used to find the terminal velocity of a bubble. The residual that will be minimized by the solver is the following:

$$\left(\frac{F_{drag}}{F_{buoyance}} - 1 \right)^2 \quad (4.37)$$

A first attempt is made with an initial guess of the terminal velocity found by Equation (4.38), where the bubble is assumed as a rigid sphere.[21]

$$v_s = \frac{2(\rho_f - \rho_p)}{9\mu} g r^2 \quad (4.38)$$

The densities indices p and f stands for particle and fluid. The solver found a solution of a terminal velocity of 0,0068 m/s for a bubble with 0,1 mm diameter. This solved terminal velocity corresponds with a

new Reynolds number of 0,96 (using Equation (4.32)) which means that the bubble can still be considered as spherical as calculated before with a terminal velocity of 0,001 m/s that served as a first guess. A typical liquid velocity is 0,5 to 1,5 m/s [25]. This means that it can be concluded that a bubble with a 0,1 mm diameter, which is of representative size in the electrode gap, has a small terminal velocity brought into relation with the velocity of the dispersion.

$$v_G = 0,0068 < 0,5 = v_L \quad (4.39)$$

The rise velocity of a single bubble is different than the rise velocity of a bubble of the same size located in a bubble swarm. The average rise velocity of a bubble swarm is always greater than that of a single bubble, thus, bubbles rise faster in swarms. An explanation for this behaviour is that a bubble is accelerated by the wake of other bubbles. For small spherical bubbles no wake has been observed. However, the swarm velocity was still observed as higher than the velocity of a single bubble.[18]

Smolianski, Haario and Luukka^[18] found a terminal velocity of 0,04 m/s for a spherical bubble in a swarm. The size of the bubbles in this swarm was not given. Anyhow, it can already be concluded that there is a difference between the terminal velocity of a single bubble and the swarm with a factor ten. The terminal velocity of a spherical bubble is particularly low compared with bubbles of different shapes.

A method where the speed of a bubble can be split up in three different parts is proposed by Nicklin [36][37]. These three parts are the superficial gas velocity, the superficial liquid velocity and a rise velocity due to the buoyancy corresponding to the swarm rise velocity (Eq.(4.40)).

$$v_{bubble \text{ in swarm}} = v_G + v_L + v_{swarm} \quad (4.40)$$

Equation (4.41) is proposed by Marrucci [35] for the calculation of the velocity of the swarm. The buoyancy due to the bubble swarm is here a function of the voidage and the velocity of a single bubble that is not located in the swarm.[8]

$$v_{swarm} = v_{single \text{ bubble}} \frac{(1-\varepsilon)^2}{1-\varepsilon^{5/3}} \quad (4.41)$$

Table 6: The extra velocity due to the swarm changes with different voidages. The value of the velocity of a single bubble is the one that is calculated earlier this chapter.

voidage	$v_{single \text{ bubble}}$	v_{swarm}
0,1	0,0068	0,0056
0,2	0,0068	0,0047
0,3	0,0068	0,0038
0,4	0,0068	0,0031
0,5	0,0068	0,0025
0,6	0,0068	0,0019

The swarm rise velocity decreases with an increasing voidage. Its relative importance compared to the velocity of a single bubble outside the swarm also decreases with an increasing voidage.

4.7 Gas voidage

In this chapter, the equation for the gas voidage will be reformed so that it can be used for the calculation of the conductivity which will in turn be used to calculate the potential in the electrode gap. The voidage describes the amount of gas in a liquid. It equals the volume of gas divided by the total volume.

$$\varepsilon = \frac{V_{gas}}{V_{gas} + V_{liquid}} \quad (4.42)$$

The voidage is a local variable and can change in space and time. At the entrance of the electrode gap the gas voidage is low since no bubbles are formed yet. It is low and not zero because there might be a small amount of bubbles that are so small that their terminal velocity is smaller than the recirculation velocity of the electrolyte which causes them to reenter the electrode gap. Further up in the electrode gap the voidage will grow gradually along the cathode until the point the flow leaves the cathode or until the limiting voidage is reached. When the current density is low, the two phase flow will still be in the homogeneous regime. All bubbles formed will then have a diameter in the same order of magnitude. Coalescence will not occur in the homogeneous regime. At a certain current density, the bubbles cannot be more closely packed without coalescence to occur; the maximum packing density is reached. Above this current density coalescence will take place which makes that bubbles with sizes of different order magnitudes will exist (see Figure 6). This is called the heterogeneous regime and it corresponds with the limiting voidage.

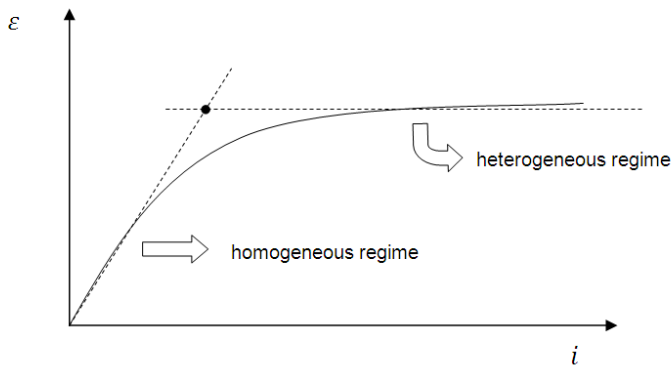


Figure 6: An increase in current density corresponds to an increasing voidage until the maximum packing density is reached. At this point the homogeneous regime, which implies the absence of coalescence, changes to the heterogeneous regime where lots of coalescence occurs.

It is important to mention that the superficial gas velocity keeps on rising alongside the cathode in upward direction. It also keeps rising with and increasing current density. The voidage will rise proportionally with this superficial gas velocity but unlike the superficial gas velocity, it will level out at a certain point which shall be called the transition point. From this transition point on, the voidage will increase no longer with an increasing superficial gas velocity, which will keep on rising with an increasing hydrogen production along the cathode. The point where the voidage stops increasing it is called the limiting voidage. [8] The

voidage stops increasing due to the transition of homogeneous regime to heterogeneous regime of the gas-liquid dispersion. In the homogeneous regime the electrolyte contains small bubbles all of the same order of magnitude. In the heterogeneous regime these small bubbles start to coalesce and break up again. This process makes that there will be both small and big bubbles in the electrolyte. Due to this coalescence the voidage will no longer increase with rising current density.

The limiting voidage is influenced by the type of the electrolyte and its concentration.[8] Factors that benefit or inhibit coalescence will also be responsible for the value of the limiting voidage. The concept of coalescence is further investigated in a separate chapter (see chapter 4.5). In this work the point of transition from homogeneous to heterogeneous regime or differently stated the limiting voidage is searched for by increasing the current density and measuring when the voidage stops increasing.

The void fraction can be estimated using the superficial gas and liquid velocities instead of the volumes of gas and liquid using the equations below. The explanation for this replacement is that if $v_{gas} \ll v_{liquid}$, which can be seen in Equation (4.39), the gas bubble can be assumed not moving compared with the dispersion velocity.

$$\varepsilon = \frac{V_{gas}}{V_{gas}+V_{liquid}} = \frac{v_{gas}}{v_{gas}+v_{liquid}} \quad (4.43)$$

$$v_g = \frac{I}{2F} \cdot \frac{RT}{P_T - P_{water}} \cdot \frac{1}{s_w} \quad (4.44)$$

$$I = i \cdot L \cdot w \quad (4.45)$$

The combination of Equation (4.44) and Equation (4.45) results in the equation below.

$$\varepsilon = \frac{1}{1 + \frac{[2 F s v_{liquid} (P_T - P_{water})]}{i R T L}} \quad (4.46)$$

The width of the electrode is denoted as w , the length as L and the distance of the electrode gap is s . When taking this into account, the cross section surface between electrodes has a surface of s_w and the surface of the electrode equals Lw . Equation (4.46) will be used in the for the calculations of the conductivity in chapter 4.8.

4.8 Conductivity and mass transfer

The value of the conductivity is important for the calculations of the cell voltage in the next chapter. Here it will be described how it is affected by the gas voidage and how it is implemented in the formula for the cell voltage.

The moment a bubble is formed at the electrode; there is an area of the electrode surface covered with H₂ gas [13]. No reaction can occur here since the reagent will not reach the electrode through the bubble. Mass transfer is also limited by hydrogen bubbles. Bubbles attached on the electrode will increase the current density, obviously, since the same current will be divided over a smaller area. The presence of bubbles in the electrolyte will affect the effective diffusivity and conductivity of the mixture. A common approach is to use the Bruggeman equation.

$$\frac{\kappa}{\kappa_0} = (1 - \epsilon_g)^{3/2} \quad (4.47)$$

The bubbles will cause the conductivity to decrease which means an extra potential drop. The lower the conductivity, the more slowly the ions in the electrolyte will move towards the electrodes. The electrons generated at the anode move over an external path with a rectifier which causes the potential difference. A higher potential difference causes higher power consumption. It is therefore wanted to keep the potential difference as low as possible. Between the anode and the cathode there is a potential drop which becomes larger with decreasing conductivities of the electrolyte which results in a potential drop. Reduction of these potential drops is very important to cut down the electricity cost of the process. The equation for the conductivity in an electrolyte is written below.

$$U = I \cdot R = I \cdot \frac{s}{A \cdot \kappa} = \frac{i \cdot s}{\kappa} \quad (4.48)$$

Table 7: The potential drop between two electrodes for current density of 2000 A/m². The Bruggeman equation predicts higher potential drops for higher voidages due to lower electrolyte resistance.

voidage	κ	U
0	37,8	0,159
0,1	32,3	0,186
0,2	27,0	0,222
0,3	22,1	0,271
0,4	17,6	0,342
0,5	13,4	0,449
0,6	9,6	0,627

Higher voidages give a lower conductivity and a higher voltage drop. This is obvious since higher voidages means more gas in the electrolyte and the conductivity of gas is lower than the conductivity of the electrolyte.

4.9 Electrode kinetics

In this chapter, the effects on the cell voltage of the bubble curtain and electrode coverage on the cell voltage will be discussed. Therefore, a short description of the Nernst and Tafel equations is given first.

4.9.1 Nernst and Tafel equation

The Nernst equation describes the equilibrium reduction potential of a half-cell in an electrochemical cell.



The molecules and/or ions and stoichiometric coefficients are respectively denoted as $ABCD$ and $abcd$. The value of z resembles the amount of electrons exchanged. The Nernst equation is written in equation (4.50).

$$U_0 = U_0^0 + \frac{RT}{zF} \ln \left(\frac{[A]^a[B]^b}{[C]^c[D]^d} \right) \quad (4.50)$$

U_0^0 is the equilibrium potential under standard conditions while U_0 is the equilibrium potential of the reaction that could be the total reaction or a half reaction. A potential is not an absolute number, it is always relative to another potential. In literature, half reactions potential is always relative to the standard hydrogen electrode (SHE) which is by convention set to zero Volt.

The overpotential (η) is a term that describes the potential difference between a half reaction's equilibrium potential, given by the Nernst equation, and the experimentally observed potential.

$$\eta = U_{exp} - U_0 \quad (4.51)$$

A non-zero overpotential is the driving force for an electrochemical reaction. The Tafel equation relates the rate of an electrochemical reaction with the overpotential. The overpotential increases with an increasing current density. In the Tafel equation it is assumed that the reverse reaction rate can be neglected in comparison with the forward reaction rate. This can only be done when the overpotential is large enough.

Anodic electrode reaction with large overpotential:

$$\eta_a = \frac{RT}{(1-\alpha)zF} \ln \frac{i}{i_0} \quad (4.52)$$

Cathodic electrode reaction with large overpotential:

$$\eta_c = -\frac{RT}{\alpha zF} \ln \frac{i}{i_0} \quad (4.53)$$

The meaning of the used symbols is denoted below.

i_0	exchange current density
i	current density
R	gas rate constant

T	absolute temperature
α	charge transfer coefficient
z	number of involving electrons at electrode
F	Faraday constant

The exchange current density is that current density when the overpotential is zero.

4.9.2 Equations governing cell potential

Three different equation will be developed now to calculate the total cell voltage. The first equation (Eq.(4.57)) ignores the effect of the bubble curtain on the voidage. The second equation (Eq.(4.67)) has the effects of the bubble curtain on the voidage implemented and in the last equation (Eq.(4.68)) electrode coverage with bubbles is implemented. Comparing the results given by these equations will give a better idea of how voidages and gas bubbles influences the potential in the electrode gap.

The total cell voltage in the chlorate process equals the sum of the voltages on the electrodes and the iR drop in the electrolyte bulk and bubble curtain (Eq. (4.54) and Figure 7).

$$U = U_a + (iR)_{bulk} + (iR)_{bubble\ curtain} + U_c \quad (4.54)$$

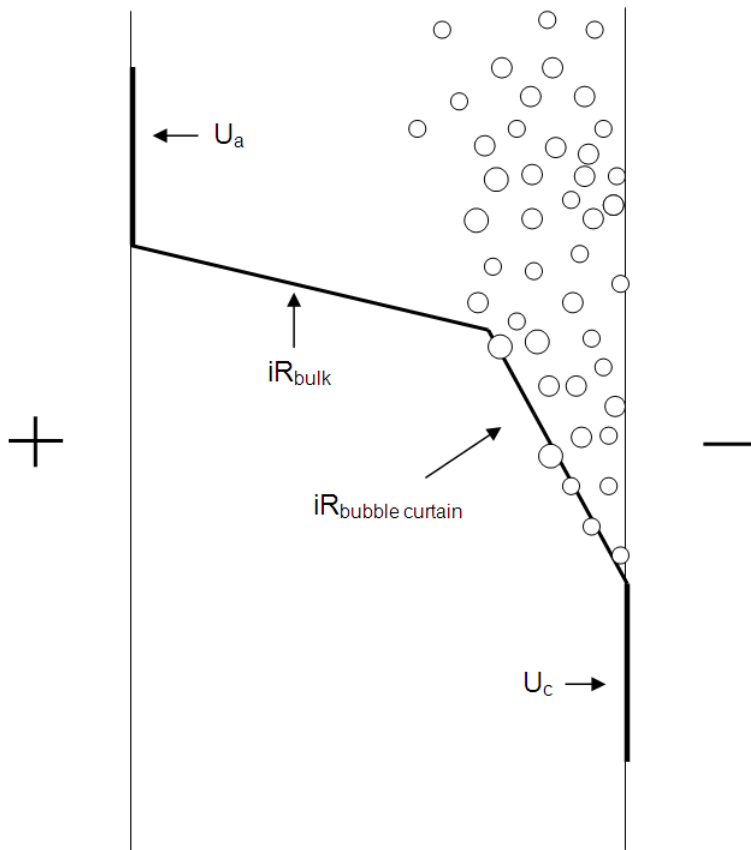


Figure 7: The total potential drop can be divided over the potential on the anode and cathode, the potential drop in the bulk and the potential drop in the bubble curtain.

First will be started for a model ignoring the bubble curtain:

$$U = U_a + U_c + iR \quad (4.55)$$

Using the Tafel equation and equation (4.48), this can be reformed to the following equation:

$$U = k_a + l_a \log(i) + k_c + l_c \log(i) + \frac{is}{\kappa(\varepsilon)} \quad (4.56)$$

The k and l constants in equation (4.56) can be retrieved in the Tafel plots or in the work of Cornell [29] for the anode and in Nyléns work [30] for the cathode. The values of k_a and l_a for the anode are respectively 0,767 en 0,121. This accounts for an aged anode and for a 550 g/L $NaClO_3$, 110 g/L $NaCl$ and 3 g/L $Na_2Cr_2O_7$ solution at pH 6,5. The temperature is 70°C and the electrode rotating rate is 3000 rpm. The current density must be ranged between 300 and 4000 A/m², since only on this interval the value for l_a is valid. [29] The values of k_c and l_c for the cathode are respectively 0,458 and 0,242. These values are also found for solution of 550 g/L $NaClO_3$, 110 g/L $NaCl$ and 3 g/L $Na_2Cr_2O_7$. The electrode was a corroded steel rotated disk electrode. The temperature also measured 70°C and the pH was 6,5.

If the bubble curtain is not taken into account, the voidage can be considered constant over the electrode gap on any certain height. Equation (4.57) below gives the expression for the voltage without a bubble curtain. The potentials found in Nyléns and Cornells work are inserted here.

$$U = 0,764 + 0,121 \log(i) + 0,458 + 0,242 \log(i) + \frac{s}{\kappa_0(1-\varepsilon)^{1,5}} i \quad (4.57)$$

The last term of equation (4.56) must be integrated if the bubble curtain is implemented in the model. Equation (4.58) is the average current density between two incremental slices. Equation (4.59) gives the incremental increase of the superficial gas velocity along an electrode surface between x_1 and x_2 .

$$\bar{i} = \frac{i_1 + i_2}{2} \quad (4.58)$$

$$v_{g2} = \frac{\bar{i}(h_2 - h_1)}{2F} \cdot \frac{RT}{P_T - P_{water}} \cdot \frac{1}{s_w} + v_{g1} \quad (4.59)$$

$$\varepsilon_2 = \frac{v_{G2}}{v_{G2} + v_L} \quad (4.60)$$

When approaching the cathode, it is presumed that the voidage increases linearly starting at distance δ (see Figure 8) since no better model is known of. The voidage in the electrolyte and the voidage in the bubble curtain are not the same. Therefore a new hypothetical voidage is introduced. It will be a combination of both the voidage in the electrolyte and in the bubble curtain. This new hypothetical voidage is found by equation (4.61). It combines both the bulk and wall voidage which are respectively denoted as ε_B and ε_W .

$$\varepsilon = \varepsilon_B + (\varepsilon_W - \varepsilon_B) \frac{x}{\delta} \quad (4.61)$$

The wall voidage is connected to the maximum packing density of the hydrogen bubbles in the bubble curtain. The maximum voidage which is the voidage at heterogeneous regime (Figure 6) is represented here as the wall voidage.

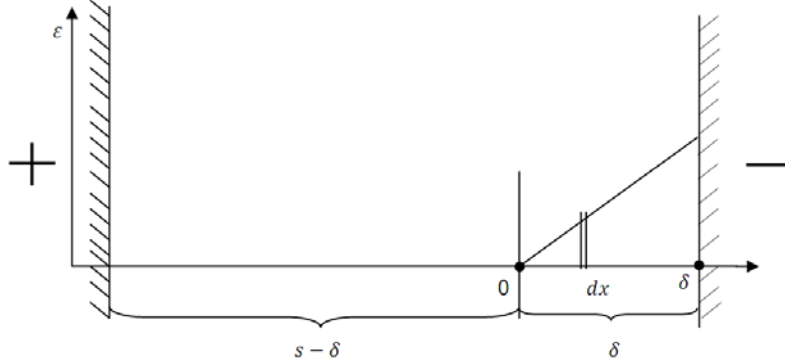


Figure 8: The voidage is considered constant in the bulk and starts increasing linearly due to the bubble curtain. The thickness of the bubble curtain is denoted as δ .

Figure 8 represents the voidage distribution in the electrode gap. At distance δ from the cathode, the bulk voidage starts increasing linearly until it reaches the wall voidages at the cathode-electrolyte interface.

$$\int_0^\delta \frac{i}{\kappa(\varepsilon)} dy = \int_0^\delta \frac{i}{\kappa_0} (1 - \varepsilon)^{-1,5} dy \quad (4.62)$$

Combining equations (4.61) and (4.62) gives:

$$\int_0^\delta \frac{i}{\kappa(\varepsilon)} dy = \int_0^\delta \frac{i}{\kappa_0} \left(1 - \varepsilon_B - (\varepsilon_W - \varepsilon_B) \frac{x}{\delta} \right)^{-1,5} dy \quad (4.63)$$

Integrating equation (4.63) will give a formula for the voidage in the bubble curtain

$$\int_0^\delta \frac{i}{\kappa(\varepsilon)} dy = \frac{-2\delta i}{\kappa_0(\varepsilon_W - \varepsilon_B)} \left[\frac{1}{\sqrt{1 - \varepsilon_B}} - \frac{1}{\sqrt{1 - \varepsilon_W}} \right] \quad (4.64)$$

$$(iR)_{total} = (iR)_{bulk} + (iR)_{curtain} \quad (4.65)$$

$$\frac{s}{\kappa_0(1 - \varepsilon)^{1,5}} i = \left(\frac{(s - \delta)i}{\kappa_0(1 - \varepsilon)^{1,5}} \right) + \left(\frac{-2\delta i}{\kappa_0(\varepsilon_W - \varepsilon_B)} \left[\frac{1}{\sqrt{1 - \varepsilon_B}} - \frac{1}{\sqrt{1 - \varepsilon_W}} \right] \right) \quad (4.66)$$

The equation with the implementation of a bubble curtain of width δ becomes

$$U = 0,764 + 0,121 \log(i) + 0,458 + 0,242 \log(i) + \frac{(s - \delta)i}{\kappa_0(1 - \varepsilon_B)^{1,5}} - \frac{2\delta i}{\kappa_0(\varepsilon_W - \varepsilon_B)} \left[\frac{1}{\sqrt{1 - \varepsilon_B}} - \frac{1}{\sqrt{1 - \varepsilon_W}} \right] \quad (4.67)$$

If δ becomes zero, which means no bubble curtain, ε_B will equal ε (see Eq.(4.61)) and equation (4.67) will become identical with equation (4.57) that neglects the presence of a bubble curtain. Including the effect of a partly bubble covered cathode, which implies an increase of the local current density gives:

$$U = 0,764 + 0,121 \log(i) + 0,458 + 0,242 \log(i/f) + \frac{(s - \delta)i}{\kappa_0(1 - \varepsilon_B)^{1,5}} - \frac{2\delta i}{\kappa_0(\varepsilon_W - \varepsilon_B)} \left[\frac{1}{\sqrt{1 - \varepsilon_B}} - \frac{1}{\sqrt{1 - \varepsilon_W}} \right] \quad (4.68)$$

A partial free area (f) is introduced in the equation above. It is the fraction of the electrode area that is not covered with adhering bubbles. It may not be mistaken with the efficiency of gas formation (f_G) introduced in chapter 4.3.

The graph in Figure 9 presents equations (4.57), (4.67) and (4.68). Equation (4.57) is used for a normal and for high liquid velocity. The reason why also a high liquid velocity is used in this equation is to make it possible to see the effect of the voidage, since a high liquid velocity will minimize the voidage.

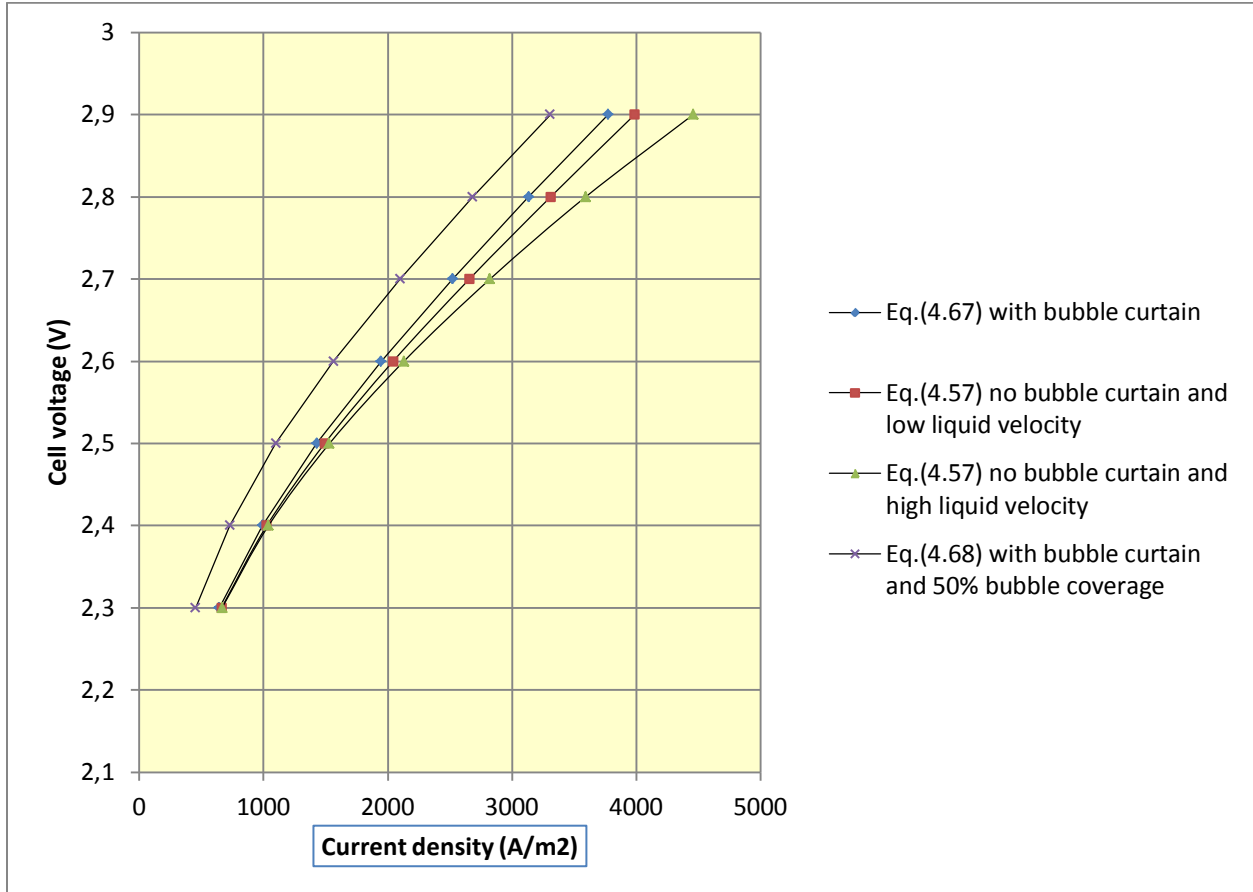


Figure 9: This graph presents the current density with corresponding cell voltage for a chlorate electrolyte under industrial conditions. The high liquid velocity is 10 m/s , wall voidage is 0,5. The other parameters can be found in chapter 4.1.

A few things can be mentioned about this graph:

The effect of the gas voidage can be seen by using a high and low liquid velocity in equation (4.57). The high liquid velocity is responsible for a very low voidage and therefore a higher conductivity (see Bruggeman equation (4.47)). This higher conductivity results in a low potential drop.

When observing the difference between the model with and without bubble curtain and a normal liquid velocity, it can be seen that the bubble curtain does have an effect on the conductivity. Higher cell

voltages are given for the model with bubble curtain compared to the model without. For lower current densities, the differences in cell voltages are getting smaller.

The implementation of a bubble curtain or high liquid velocity will almost have no effect on the cell voltage for low current densities. The biggest change in cell voltage occurs when bubble coverage on the cathode is taken into account. Of course this depends on the value of the coverage on the cathode which was taken as 0,5 here. Keeping the cathode surface free from bubbles has a higher impact on the total cell voltage than increasing the liquid velocity to reduce the voidage.

In reality, the voidage, bubble curtain and bubble coverage are all effecting the cell voltage together. The developed Equations serve to figure out their mutual importance. Different values can be used for the parameters in the Equations to see their influence. Learning more about how the cell voltage is influenced by different parameters will help to find a way to reduce the cell voltage or at least point out where the biggest changes can be made.

4.10 Dissolving time of a small bubble

Close the cathode only small bubble appears as seen in Bollens work.[1] Further away from the cathode the bubbles are larger (see Figure 10). Since coalescence does not occur, there must be another explanation on how those larger bubbles of the size of 0,1 mm can exist and where they come from.

Once a bubble is formed, it gets bigger by diffusion and absorption of hydrogen from the liquid into the bubble [13]. The larger a bubble becomes, the slower it can grow because the area/volume ratio is getting smaller with a larger volume. The larger a bubble, the lower its inside pressure (see Eq.(4.10)). A large bubble will absorb the hydrogen from a smaller bubble through the electrolyte because of the difference of Laplace pressure of two bubbles of different size. The pressure gradient can be seen as the driving force of the mechanism where a larger bubble will absorb the hydrogen from a smaller bubble. This explains why larger bubbles only appear further away from the cathode since then they already had time to grow. The speed at which the diameter of a dissolving bubble decreases is calculated. Together with the diameter of the bubble, this speed will result in a certain time it takes for a big bubble to fully dissolve a smaller bubble. Of course this way of reasoning is only acceptable if there is a large bubble near the cathode and close enough to the small bubble.

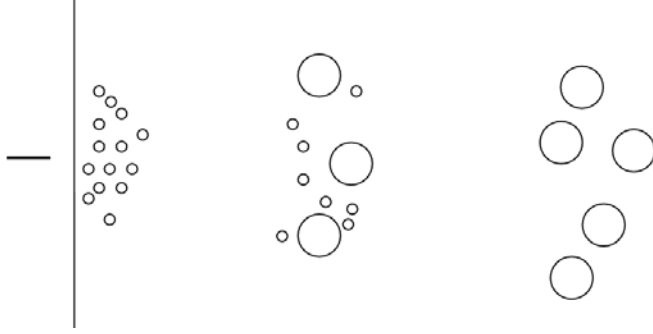


Figure 10: Small bubbles are formed close to the cathode, further away from the cathode more larger bubbles are seen.

It is assumed here that all occurring mass transfer is happening by diffusion. There is one small bubble in contact with the solution that is kept at an equilibrium hydrogen concentration that is maintained by an undetermined number of ever present larger bubbles of a certain equilibrium size. A very small bubble can be considered as rigid, therefore its Sherwood number will approach 2. [21]

$$Sh = \frac{k_m d}{D} = 2 \rightarrow k_m = \frac{2D}{d} \quad (4.69)$$

$$\dot{n} = k_m A \Delta c \quad (4.70)$$

$$(P_{inside} - P_{outside}) = \frac{2\sigma}{r} \quad (4.71)$$

$$P_{H_2} = \frac{4\sigma}{d} + P_{out} - P_{water} \quad (4.72)$$

Considering the Laplace pressure and knowing that the total pressure can be split up in the hydrogen and water pressure, equations (4.73) and (4.74) can be derived below. Also the hydrogen solubility in a sodium chlorate solution (Table 2) is used here.

$$c_1 = S \cdot \left(\frac{4\sigma}{d_1} + P_{out} - P_{water} \right) \quad (4.73)$$

$$\Delta c = c_1 - c_2 = S \cdot 4\sigma \left(\frac{1}{d_1} - \frac{1}{d_2} \right) \quad (4.74)$$

Index 1 and 2 corresponds respectively to a small and large bubble. The big bubble will suck up the hydrogen of the smaller bubble due to the pressure gradient. The combination of Eq.(4.69), Eq.(4.70) and Eq.(4.74) results in Eq.(4.76).

$$\dot{n}_{H_2} = k_m A \Delta c = \frac{2D}{d_1} \cdot 4\pi \left(\frac{d_1}{2} \right)^2 4 S \sigma \left(\frac{1}{d_1} - \frac{1}{d_2} \right) \quad (4.75)$$

$$\dot{n}_{H_2} = 8 S D d_1 \pi \sigma \left(\frac{1}{d_1} - \frac{1}{d_2} \right) \quad (4.76)$$

The following equation is the amount of mole hydrogen in a bubble in function of the diameter. The next step is to derivate this equation to the time. By doing this a second equation for the flux is calculated (Eq.(4.78)).

$$n_{H_2} = \frac{PV}{RT} = \frac{\frac{4}{3}\pi\left(\frac{d_1}{2}\right)^3 \left(\frac{4\sigma}{d_1} + P_{out} - P_{water}\right)}{RT} \quad (4.77)$$

$$\dot{n}_{H_2} = \frac{\frac{4}{3}\pi\sigma d_1 + \frac{1}{2}\pi(P_{out} - P_{water})d_1^2}{RT} \frac{d(d)}{dt} \quad (4.78)$$

Both equations for flux (Eq. (4.76) and Eq.(4.78)) are combined and the speed in which the diameter decreases while the bubble dissolves is found in equation (4.79). Dividing the bubble diameter by the speed of diameter decrease will give a rough estimate of the time it takes for a bubble to dissolve (Eq.(4.80)). The speed increases for smaller diameters so the actual dissolving time will be shorter than the time calculated by Equation (4.80). A more accurate way of calculating the dissolving time would therefore be to use integrals.

$$\frac{d(d)}{dt} = \frac{8SDd_1\pi\sigma RT\left(\frac{1}{d_1} - \frac{1}{d_2}\right)}{\frac{4}{3}\pi\sigma d_1 + \frac{1}{2}\pi(P_{out} - P_{water})d_1^2} \quad (4.79)$$

$$time = \frac{d_1}{d(d)/dt} \quad (4.80)$$

Table 8: The dissolving time and speed for several bubble sizes in the vicinity of a 0.1 mm bubble.

d1	d2	d(d)/dt	Dissolving time (s)
3,33E-05	0,0001	4,20E-07	79
1,00E-05	0,0001	5,52E-06	1,81
3,33E-06	0,0001	3,97E-05	0,084
1,00E-06	0,0001	2,37E-04	0,0042
3,33E-07	0,0001	9,12E-04	0,0004
1,00E-07	0,0001	3,37E-03	0,00003

The time it takes to dissolve small bubbles have to be compared with the residence time in the electrode gap. Bubbles with a diameter of 1 μm and smaller have a very low buoyancy but high drag force and will therefore not have a significant terminal rise velocity. The residence time in the electrode gap can then be calculated by dividing the length of electrode by the liquid velocity as seen in the equation below.

$$residence\ time = \frac{electrode\ length}{v_L} = \frac{0,5\ m}{0,5\ m/s} = 1\ s \quad (4.81)$$

It can be seen in Table 8 that the time it takes for a bubble with a diameter of 1 μm is very small compared to the calculated residence time of 1 second. The time that small bubbles remain in the electrode gap is long enough to be fully dissolved by larger bubbles in the vicinity. It can be concluded that very small bubbles formed at the cathode (see chapter 4.4) have time enough to dissolve and the larger bubbles near will absorb the hydrogen. It takes time to migrate for bubbles from the cathode further into the bulk. In this time, small bubbles will dissolve and other larger bubbles will grow by absorbing the hydrogen of the smaller dissolving bubbles. This explains why close the cathode more small bubbles are seen and further away less smaller and more larger bubbles.

Table 9: The volume of a bubble with the required dissolving volume for different bubble sizes. Also the factor difference between these two volumes is given.

d (meter)	V_{bubble} (m³)	Dissolving liquid V (m³)	factor difference
1,00E-04	5,24E-13	9,34E-11	178
1,00E-05	5,24E-16	1,02E-13	194
1,00E-06	5,24E-19	1,23E-16	234
1,00E-07	5,24E-22	1,31E-19	250
1,00E-08	5,24E-25	1,32E-22	252

Table 9 shows the volume needed to dissolve a bubble with certain diameter. The concentration at which the bubble will be dissolved is the saturation concentration of the bubbles original size (see Table 3). The size of the bubble has an influence on the volume of liquid it takes to dissolve the whole bubble. For smaller bubbles the hydrogen pressure increases while the water pressure remains the same which means that the ratio hydrogen over water inside the bubble will increase. A small bubble requires about 200 times its own volume in hydrogen free electrolyte to be fully dissolved.

A gas voidage where the volume of gas is 200 times lower than the liquid volume is about 0,005 which is much lower than voidages under industrial conditions of about 0,4. Therefore, there will not be enough liquid around for all the small bubbles to dissolve. This means that before a small bubble is fully dissolved, much of the already dissolved hydrogen will already be absorbed by bigger bubbles in the vicinity. Dissolving of smaller bubbles goes along with absorbing of hydrogen for the larger bubbles.

4.11 Hydrogen Transport

Newly produced hydrogen at the cathode can be transported away in three different, simultaneously occurring ways. These are diffusion, transport in bubble form, and convection (Eq.(4.82)). The order of magnitude of these three terms will be calculated to get a better understanding of which terms are dominant. Many assumptions are made so these values can only be seen as a very rough estimation, depending on what assumptions are made.

$$\dot{n}_{H_2} = D \frac{dc_{H_2}}{dz} + \dot{n}_{bubbles} + v c_{H_2} \quad (4.82)$$

The flux of hydrogen produced at the cathode can be calculated out of the current. (Eq.(4.4))

$$\dot{n}_{H_2} = \frac{i}{2F} = \frac{2000}{2 \cdot 96\,485} \cong 0,01 \frac{mole}{s \cdot m^2} \quad (4.83)$$

The diffusion term is calculated with the boundary layer thickness dz that can be found by Equation (4.25). A bulk concentration of $0,12 \text{ mole}/m^3$ is found in Table 3 for a bubble of $0,1 \text{ mm}$ which is a typical bubble size in the bulk [1]. A bubble right at the cathode has an estimated size of $1 \mu m$ which corresponds to a saturation concentration of $0,49 \text{ mole}/m^3$.

$$D \frac{dc}{dz} = 6,73 \cdot 10^{-9} \frac{0,49-0,12}{7,49 \cdot 10^{-5}} = 3,32 \cdot 10^{-5} \frac{mole}{s \cdot m^2} \quad (4.84)$$

The amount of hydrogen transported by diffusion is much smaller than the total flux calculated in Equation (4.83). Of course, if this estimated bubble at the cathode is two orders of magnitude smaller, the saturation concentration at the cathode would be much higher and then the diffusion term would be higher too. This means that the importance of this estimation of a $1 \mu m$ bubble size on the results may not be ignored.

Hydrogen leaving the cathode in a bubble appearance corresponds to the $\dot{n}_{bubbles}$ term. A bubble at the cathode with an estimated size of $1 \mu m$ corresponds to an internal pressure of $3,7 \text{ bar}$. In the equations below the speed of hydrogen being removed from the cathode is calculated assuming that all the hydrogen transport occurs by bubble formation.

$$c_G = \frac{P}{RT} = \frac{3,7 \cdot 10^5}{8,31 \cdot 343} = 123 \frac{mole}{m^3} \quad (4.85)$$

$$v = \frac{\dot{n}_{H_2}}{c_G} = \frac{0,01}{123} = 8,1 \cdot 10^{-5} \frac{m^3}{s \cdot m^2} \quad (4.86)$$

$$v = 0,081 \frac{Liter}{s \cdot m^2} = 0,081 \frac{mm}{s} \quad (4.87)$$

Small bubbles with a diameter of $1 \mu m$ will detach from the nucleation point. These bubbles have a very low buoyancy but high drag force and will therefore not have significant terminal rise velocity. So when these small bubbles detach from the cathode, they will move horizontally away from the cathode which results in convection.

The convection term vc_{H_2} is calculated with the bubble speed removal from the cathode in Equation (4.86). It is assumed here that most of the hydrogen removal occurs by convection which makes that the real value of the velocity in Equation (4.86) will be lower since the fraction of the flux resulting in bubbles will be lower than 0,01.

$$vc_{H_2} = 8,1 \cdot 10^{-5} \frac{m}{s} \cdot 0,49 \frac{mole}{m^3} = 4 \cdot 10^{-5} \frac{mole}{s \cdot m^2} \quad (4.88)$$

The amount of hydrogen transported by convection is much smaller than the total flux calculated in Equation (4.83).

Since both diffusion and convection are too low to remove all the hydrogen formed at the cathode, at least for the assumption of a $1 \mu m$ bubble at the cathode, it can be concluded by deduction that hydrogen removal in bubble form ($\dot{n}_{bubbles}$) will be the dominating term in Equation (4.82) for a current density of $2000 A/m^2$. If the estimated bubble size at the cathode will be smaller than $1 \mu m$ then will both the convection and the diffusion term will increase since they are proportional with the saturation concentration at the cathode. The current density is correlated with the convection term and the bubble term while the diffusion term is not. Therefore, a decrease in current density will make the role of diffusion more important compared to the other two terms. This is also concluded by Vogt [13] who says that an increasing current density will result in a higher efficiency of gas evolution which means a more dominating.

With the assumptions made, hydrogen will leave the cathode mostly in bubble form. Anyhow, in the end, all the hydrogen will leave the electrolyte in bubble form.

Chapter 5. Experimental

In the work of Bollens [1] small bubbles and coalescence inhibition was observed. In the experiments done here, more information about the point where coalescence starts occurring and the maximum voidage was searched for. In doing this, a device was made that makes it possible to work under industrial conditions. For a certain electrolyte composition, where both temperature and pH can be regulated, the current density was increased stepwise.

5.1 Equipment

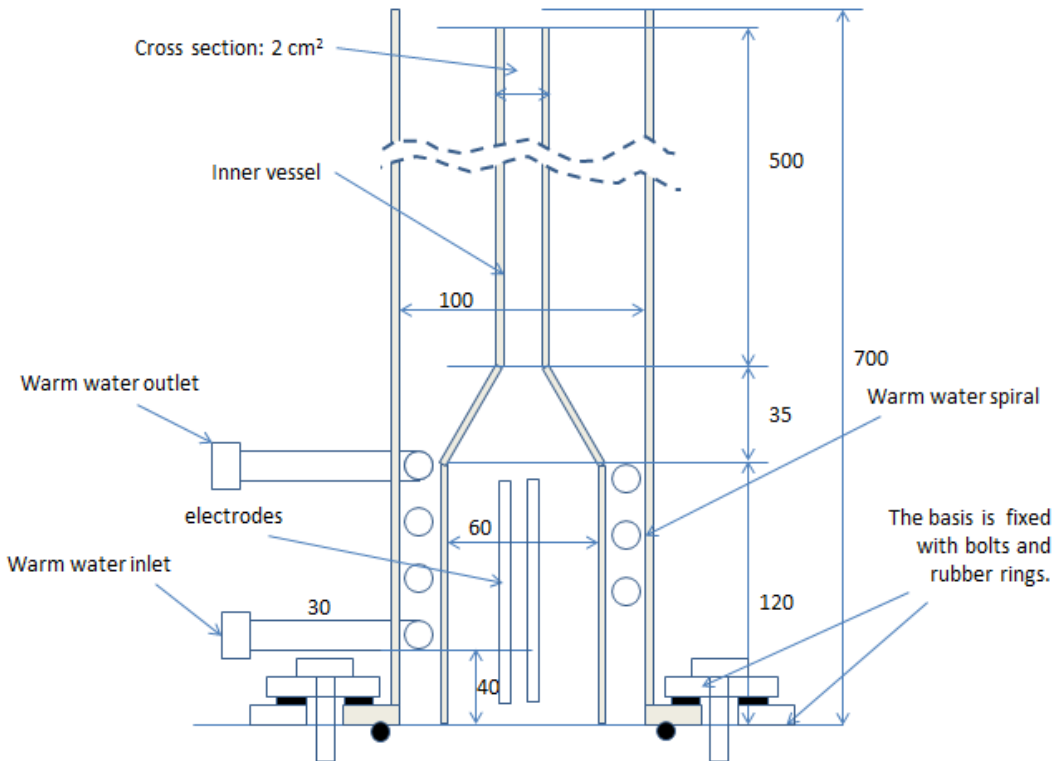


Figure 11: The equipment used and depicted here are an inner and outer tube, spiral linked with warmwater bath, basis fixed with bolts and rubber rings. The hoses and pH meter entering the system from below are not depicted here. The numbers in the drawing are a length and their unit is mm.[41]

Figure 11 shows the experimental setup. The outer vessel is a cylindrical tube with a diameter of 10 cm and it is made of glass. The inner vessel is also made of glass; the lower part of which has a diameter of 6 cm while the upper part has a cross section of 2 cm². The lower part is wider because space is needed to generate bubbles under industrially relevant conditions and to control the pH which otherwise would increase since chlorine escapes and unreacted hydroxide would remain. The upper part, the riser tube, is much thinner in order to obtain a higher voidage which can be measured more easily. The same amount of bubbles rising in a thinner tube will give higher voidages. The grading at the upper part of the inner vessel corresponds with two mL for every cm in height. The volumes of electrolyte inside the inner vessel and in between the inner and outer vessel are communicating.

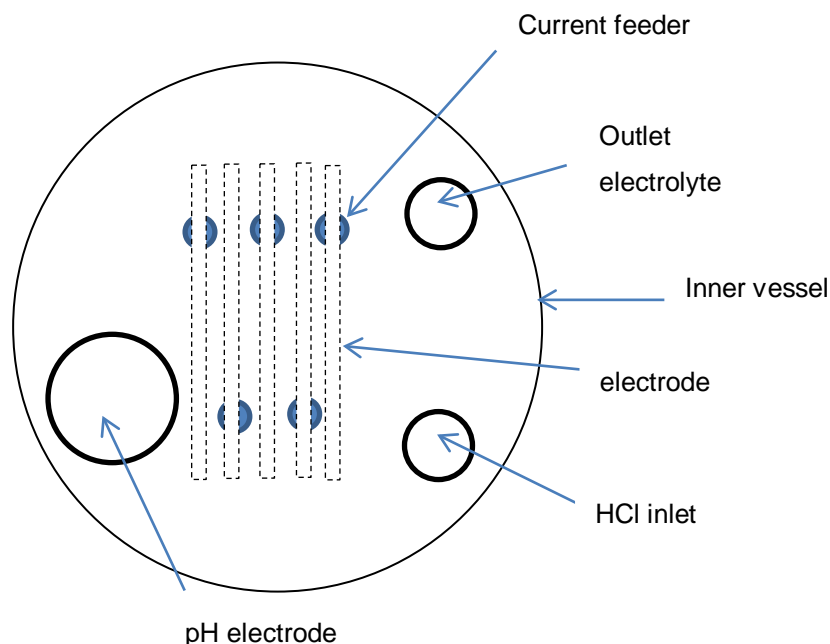


Figure 12: Top view of the inner vessel. The position of the pH electrode, anodes and cathodes, electrolyte outlet and HCl inlet are all located inside the inner vessel. The blue dots are the current feeders to the electrodes.

All the different inlets and electrodes that enter the system from beneath are depicted in Figure 12. A maximum of five electrodes can be installed. Every electrode measures 3 by 5 cm. These electrodes are equally spaced, planar and vertically positioned. The anode was a Dimensionally Stable Anode (DSA electrode). It is used in all chlor-alkali and chlorate plants. It consists of a 10 μm electro catalytic coating of $\text{Ru}_x\text{Ti}_{1-x}\text{O}_2$. Under industrial conditions a steel cathode is used. In this experiment a titanium cathode is used in order to avoid corrosion. A rectifier is used to set the wanted magnitude of the current between the electrodes.

The pH electrode (Mettler Toledo InPro®3100 UD/120/Pt1000) is applied from below which is quite unusual. This electrode also contains a Pt1000 temperature sensor. The pH electrode was calibrated with commercial 4.0 and 7.0 buffers at room temperature and is interconnected with the HCl pump. Whenever the pH rises, then HCl will be pumped through the HCl inlet to adjust it. Plastic curtains are placed around the rack beneath the system, there where the electrodes and HCl enters. This is done for safety reasons in case the HCl inlet gets loose. The thermostat bath is connected with spirals inside the outer vessel to keep the system at the desired temperature. The thermostat bath is not regulated by the temperature sensor in the pH electrode. To empty the reactor after usage another hose is installed through the bottom of the reactor. The pH electrode with temperature sensor, HCl pump and rectifier are connected to a computer where data are logged.

Above the electrolyte in the vessel there is a hose with air flow to dilute the hydrogen leaving the electrolyte. Hydrogen gas and air becomes an explosive mixture when the concentration of hydrogen exceeds 4%. On top of the vessel a suction cap is placed to remove the formed and already diluted hydrogen as an extra precaution.



The following chemicals are used:

-*NaCl*

-*NaClO₃*

-*HCl*

-*Na₂Cr₂O₇*

A brief risk analysis of these products can be found in the addendum.

5.2 Procedure

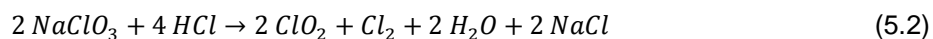
The experiment is done by increasing the current since the electrode surface remains constant. First one liter of electrolyte is used during the experiment. Then it is repeated with two and three liters of electrolyte by adding one extra liter in the next trial. The amount of electrodes and their size can be changed in between two separated experiments. This means it might be possible to have a different current density for the same current. In the first attempts the warm water bath will maintain a temperature of 32°C.

The consecutive steps in the experiment are:

1. The reactor is cleaned with water.
2. The thermostat bath is started. Check if the water volume is sufficient.
3. The ventilation suction is checked with a strip of paper.
4. If needed, the *pH* electrode is recalibrated with buffer 7 and 4 at room temperature.
5. The *HCl* valve is closed.
6. The bottom drainage function is checked with water.
7. The stipulated volume of chloride/chlorate electrolyte is prepared by dissolving the salts in hot, deionized water. Dichromate is added together with double the molar amount of sodium hydroxide to convert the dichromate to chromate.
8. Electrolyte is charged to the reactor and temperature equilibrium is awaited.
9. The inner vessel and the off gas suction hood are put in place.
10. The computer is started with pH settings according to plan.
11. A minimum through flow of 6 Nl/min air must continuously flush the headspace. To avoid explosive gas mixtures the maximum current for 6 Nlpm is 30 A. 10 Nlpm permits 50 A.
12. The *HCl* valve is opened.

13. The electrical current is increased in small steps until the volume expansion levels out. The levels of the inner and out vessels are tabulated together with the current.
14. The final electrolyte volume is measured and the concentration changes of chloride and chlorate are determined.
15. The *HCl* valve is closed.
16. The apparatus is emptied and a sample is saved for possible analyses.
17. The equipment is cleaned with water.
18. If the pH electrode is left in the apparatus, it should be covered under about 1 dm water and closed top lid.
19. If necessary, physical data are determined for the sample.

During the experiment hydrochloric acid (*HCl*) is added to maintain the *pH* at the premised level. Right at the inlet of the *HCl* its concentration will be rather high and the following side reaction will occur.



An important drawback of this reaction is the formation of chlorine dioxide (*ClO₂*) which is explosive at concentrations with partial pressures above 0,1 bar. A more extensive risk analysis can be found in the addendum.

5.3 Results and discussion

Table 10 and Table 11 present the results for two and three liter electrolyte. This gave levels of 32 and respectively 44 mL above the starting level where the voidage was zero. In both cases two electrodes are used, which means there was one electrode gap of 15 cm^2 .

Table 10: The results of an electrolysis with a 2 liter solution of **500 g/L NaClO₃**, **100 g/L NaCl**, **1.5 g/L NaOH** and **5 g/L Na₂Cr₂O₇**. Two electrodes are used.

Time (min)	Amps	T (°C)	pH	lvl (mL)	ε riser	ε tot	v (m/s)
19	0	34,1	8,15	76	0,00	0,000	0,0000
20	2	34,6	8,4	72	0,14	0,009	0,0013
22	5	33,9	8,51	67,4	0,26	0,020	0,0033
25	10	33,1	8,07	44	0,57	0,071	0,0065
29	15	34,6	7,92	43	0,58	0,073	0,0098
32	20	36,3	7,68	45	0,56	0,069	0,0132
34	25	38,7	7,49	44	0,57	0,071	0,0166

Table 11: The results of an electrolysis with a 3 liter solution of **500 g/L NaClO₃**, **100 g/L NaCl**, **1.5 g/L NaOH** and **5 g/L Na₂Cr₂O₇**. Two electrodes are used.

Time (min)	Amps	T (°C)	pH	lvl (mL)	ε riser	ε tot	v (m/s)
38	0	34,4	8,86	50	0,00	0,000	0,0000
39	2	33,9	8,65	45	0,09	0,011	0,0013
41	5	33,3	8,6	39,6	0,17	0,023	0,0033
43	10	32,9	8,26	17,6	0,39	0,068	0,0065
47	15	33,9	7,91	10	0,44	0,082	0,0098
50	20	35,7	7,67	6	0,47	0,090	0,0131
53	25	38,4	7,76	4	0,48	0,093	0,0166

The pH is rather high because the *HCl* pump was not turned on since it was forgotten to turn it on. The time in minutes is given to see the relevant timespan between two measurements, which about two or three minutes.

Voidage is zero without current, obviously since no hydrogen is formed. The total volume of the inner vessel measures 496 mL while the volume of the riser tube only measures 100 mL. By calculating the total voidage the volume of the lower part of the vessel was included while for the calculation of the voidage of the riser tube ignores the volume of the lower part of the inner vessel.

The voidage is calculated out of the level of the electrolyte that can be measured on the inner vessel. The voidage in the riser tube equals the amount of gas in the system divided by the total amount of liquid and gas together in the riser tube. The total voidage equals the total amount of gas divided by the total amount of liquid and gas in the inner vessel. The total amount of gas is the difference of the level that can be seen on the riser tube with and without a current. The level is a method of describing the total amount of mL in the system.

The total voidage inside the inner vessel can be divided into two different voidages. The first is the void fraction from the riser tube which is the part with a cross section of 2 cm^2 . The other void fraction is the one in the lower part under the riser tube which is not tabulated. It is important to see that there is a difference between these two voidages. It is assumed that when the voidage of the riser tube levels out that also the total voidage is levelled out. The last column in Table 10 and Table 11 contains the superficial gas velocity through the riser tube using equation (4.5) with the cross section of the riser tube:

$$v_g = \frac{I}{2F} \cdot \frac{RT}{P_T - P_{\text{water}}} \cdot \frac{1}{A_{\text{cross section}}} \quad (4.5)$$

This superficial gas velocity describes the velocity of both hydrogen and water gas.

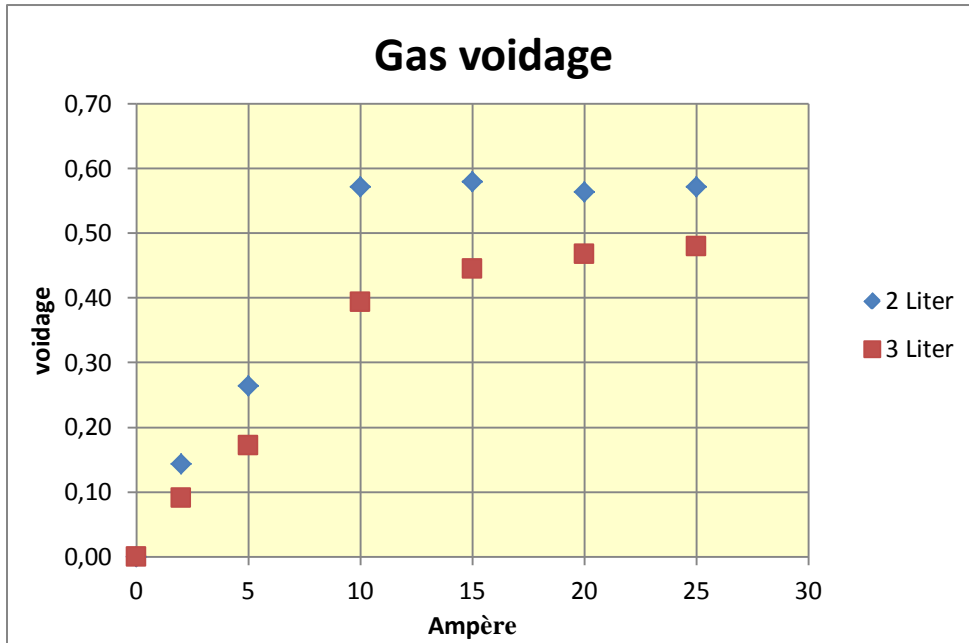


Figure 13: The y-values are the voidages in the riser tube in Table 10 and Table 11. The x-values are the current. These results are for one electrode gap with electrodes measuring 3 by 5 cm. The 2 and 3 liter resembles the total amount of electrolyte poured in the bubble reactor.

It can be seen in Figure 13 that the voidage levels out around 10 A which corresponds to a superficial velocity of $0,0065 \text{ m/s}$ and that there is a limiting voidage just as it was expected. The current density was not reported since half of the electrode surface is located outside the electrode gap. The difference in voidages for the same current is obvious since the same amount of gas is produced for the same current but the amount of electrolyte differs.

Even though the gas voidage levels out, the bubbles did not behave as expected. Directly after starting the reactor, it was possible to see a bubble induced volume increase that seemed to level out when a transition point current was exceeded. However, the bubbles were about ten times larger than those observed in Bollens' studies [1] and it must be concluded that coalescence was occurring.

The cause of the early coalescence is most likely the walls of the converging section between the upper and lower zones.

The results of the experiment did not fulfill the expectations that no coalescence should occur on the wall. The bubble beds were unstable and collapsed. The bubbles in the bed were several millimeters due to coalescence. Therefore, an alternative way has been searched to get rid of the coalescence under same circumstances. The inner tube was replaced by another straight tube of 6 cm in diameter; just the same diameter as the lower part of the previous inner tube, but this time the diameter remained the same over the whole distance of the tube. Since there was no longer a converging section which might explain the occurring coalescence, it was hoped that coalescence would occur no more. The disadvantage of this wider tube was that higher current densities were required to obtain measurable void fractions. At 50 A there was a black smoke evolution and the experiment had to be stopped. There was high heat production at the point where the electrodes entered the system through the plastic bottom. This plastic bottom started to melt as can be seen in Figure 14.

There was no time available to repair and modify the setup so the experiments had to be interrupted at this point.

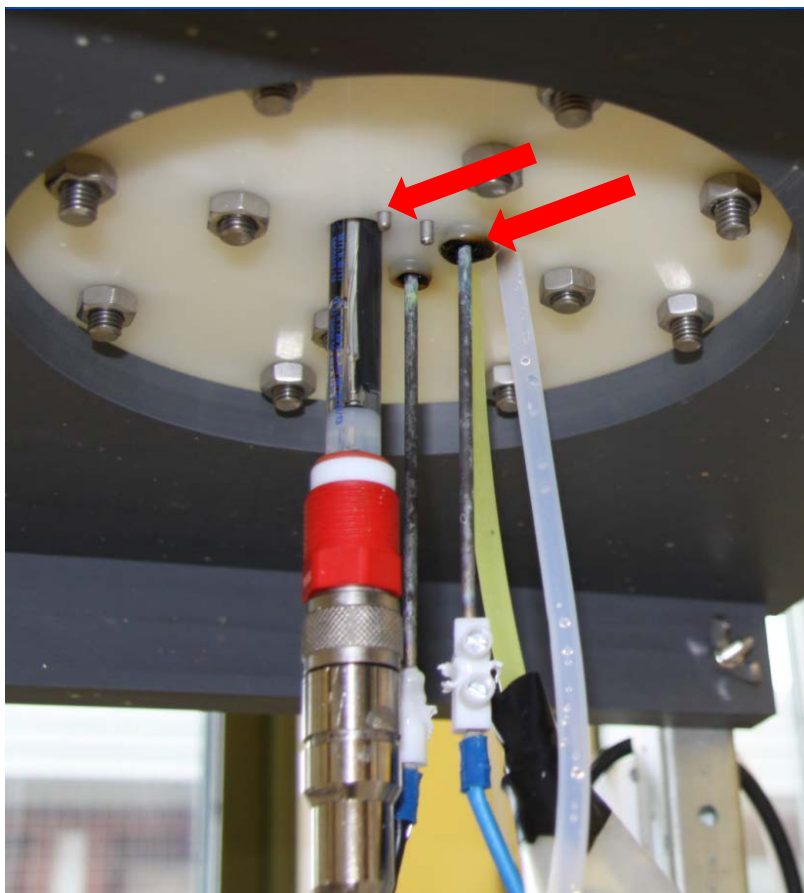


Figure 14: The two red arrows show an unused electrode connection and an electrode connection where melting and burning occurred.

Chapter 6. Conclusion

Bubble formation: Chlorate electrolysis has been studied theoretically and experimentally under industrial relevant conditions. The electrolyte had a composition of 8% and 43% of chloride and chlorate and had a temperature of 70°C.

A theoretical analysis shows:

- Bubbles in the electrode gap are spherical shaped and may have sizes in range of $3,2 \cdot 10^{-9} \text{ m}$ to $0,1 \text{ mm}$.

- Theoretically, extremely small bubbles ($3,2 \cdot 10^{-9} \text{ m}$) can be formed at the cathode, with a size depending on the saturation concentration of hydrogen. This saturation concentration is dependent on the efficiency of bubble formation and mass transfer. This minimum bubble size at the cathode causes an extra potential drop.

- The order of magnitude of the boundary layer at the cathode ($7,5 \cdot 10^{-5} \text{ m}$) is larger than the minimum possible bubble size at the cathode but it is about the same as the average bubble size in the bulk.

- The dissolving time of a small bubble ($1 \text{ }\mu\text{m}$) with a larger bubble ($0,1 \text{ mm}$) in the vicinity, with the pressure difference in the two bubbles as driving force, is small ($0,0042 \text{ s}$) compared with the residence time of the electrolyte in the electrode gap (1 s). This small bubble will have the time to be fully dissolved since larger bubbles in the vicinity surround themselves with a lower hydrogen concentration than small ones. This explains why further away from the cathode less small bubbles are seen, since they dissolve while migrating away from the cathode.

- A bubble requires about 200 times its own volume in hydrogen free liquid to dissolve. Since only a very low voidage would offer enough liquid volume, it can be concluded that before a small bubble is fully dissolved absorption of hydrogen into larger bubbles will already take place.

- Bubble coverage on the cathode increases the cell voltage since it increases the local current density. It may affect the cell voltage more than the voidage or the bubble curtain does. In reality, it is the combination of the voidage, the bubble curtain and the bubble coverage that will all together increase the cell voltage. The developed Equations can be used to show relative importance of these different factors.

Extremely small bubbles can exist at the cathode. These small bubbles will dissolve and be absorbed by larger growing bubbles. Since there is both time and a driving force for the dissolving of small bubbles, there will no longer exist very small bubbles further away from the cathode. They will be dissolved and absorbed by larger growing bubbles. This process explains why larger bubbles exist, since they are not formed by coalescence.

The experiments were made with electrochemical bubble formation on vertical electrode surfaces in electrolyte of composition 500 g/L NaClO_3 and 100 g/L NaCl and temperature of about $35\text{ }^\circ\text{C}$. The voidage of water saturated with hydrogen was studied by measuring the volume expansion in a vertical tube of $14,1\text{ mm}$ diameter.

Under the experimental conditions, it can be concluded that:

-The voidage levels out at a certain voltage and a maximum packing density is found. In the first experiment where 2 L of electrolyte is used, the maximum voidage with respect to the inner tube volume was $0,57$ and for the second experiment with 3 L of electrolyte used, it was $0,39$. These values are not compensated for gas voidages in the bottom section of the inner vessel. In both cases the transition point from homogeneous to heterogeneous regime was around 10 A . For this current a superficial gas velocity with respect to the cross section of the riser tube of $0,0065\text{ m/s}$ accounts.

-The bubbles observed did coalesce and the bubble bed was not stable. The level of the bed was fluctuating constantly due to all the occurring coalescence. The bubbles in the bed were several millimeters long.

Chapter 7. **Recommendations**

The packing density should be measured in an experimental setup where no coalescence occurs and no heat evolution occurs.

The experiment in this work should be redone in a way where no experimental breakdown occurs. Large heat production at the point where the electrodes enter the system must be prevented. The current feeders can be made larger so that there will be less heat production. Another possibility is to apply an isolator between the current feeders and the plastic bottom.

The converging walls in the inner vessel between the lower part and the riser tube can be made longer, so that the converging parts are less steep. By this it might be possible to reduce the coalescence.

Chapter 8. Addendum

Risk analysis

Risks	Consequence	Action
Heat	Getting burnt	Clothes, gloves
Hydrogen	>4% H ₂ in air can cause explosion >4% O ₂ in H ₂ gives explosion	>5 L/min air -usage of suction cap
Nitrogen	-unconsciousness -death	-minimise usage -use during start up -usage of suction cap
leakage	-hit people -mess -destroy electrical components	-leak test with water -encapsulate with foil
electricity	-destruction of equipment -fire -short-circuiting -heat evolution	-avoid short-cutting -never use under designed equipment

All the actions taken in an attempt to minimize or prevent risky behaviour has to be checked by an independent person.

Chemicals	Risk	Consequence
Na ₂ Cr ₂ O ₇	poison	carcinogenic
NaClO ₃	Fire	Equipment damage personal damage
NaOH	damage on eyes and skin	personal damage
HCl	damage on eyes and skin	personal damage

The best way of protection against these chemicals, and all chemicals in a general sense, is to wear special protection glasses and clothes. The glasses have to be closed on the sides, above and below. Clothes, shoes and gloves protects against direct contact. Chlorate can also impregnate clothes or shoes without noticing. Clothes or shoes can then ignite at any time and can therefore only be worn in the lab. It is in this place that emergency showers and fire blankets are always near. If impregnated clothes or shoes would ignite elsewhere, it would be a lot more dangerous for one self.

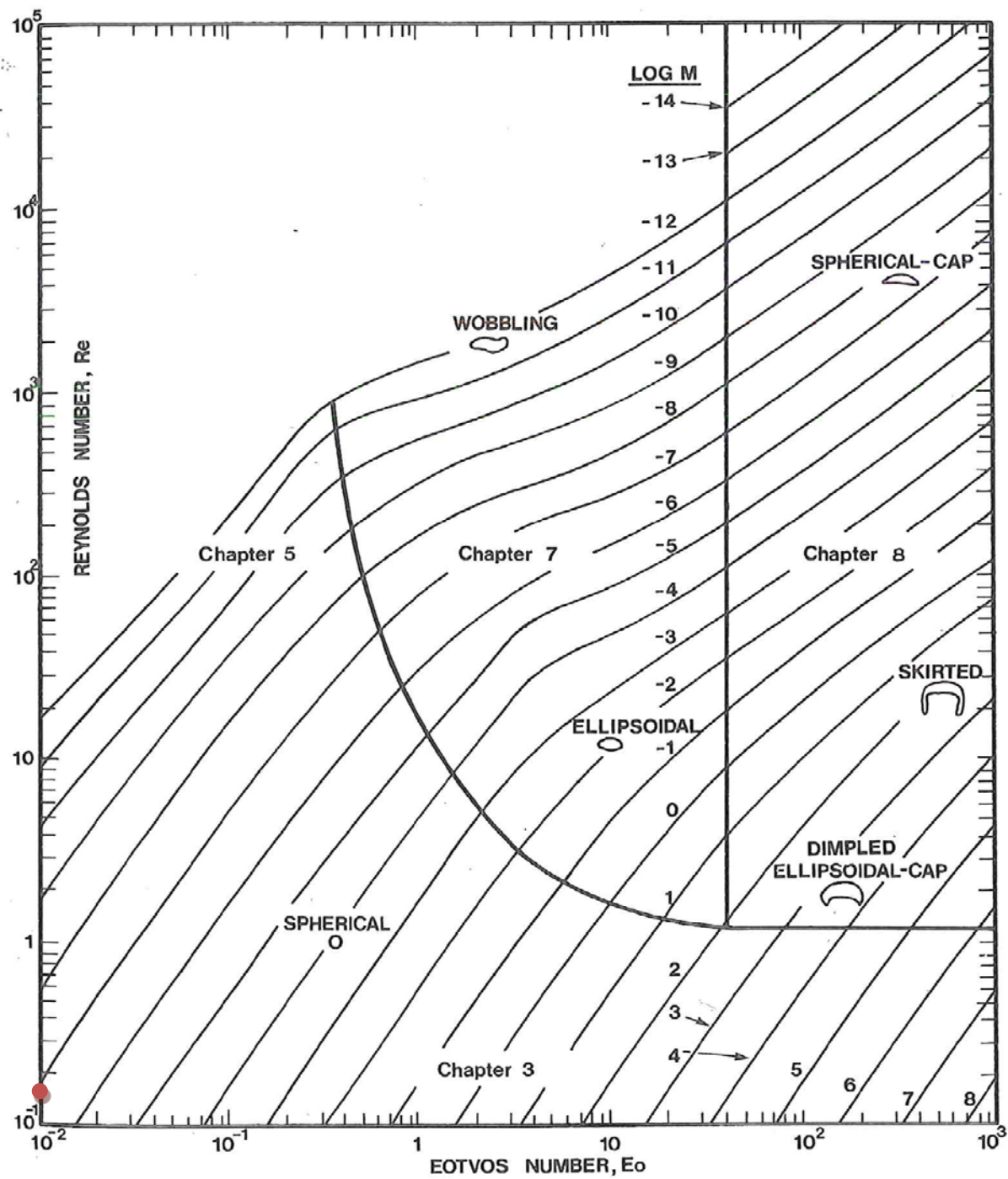


Figure 15: This diagram divides bubbles with different shapes depending on Reynolds and Eötvös number bubbles. The red dot corresponds for the Reynolds and Eötvös number for a bubble of 0.1 mm (Table 5) and can be considered spherical. [21]

Påtvångad strömning i rör

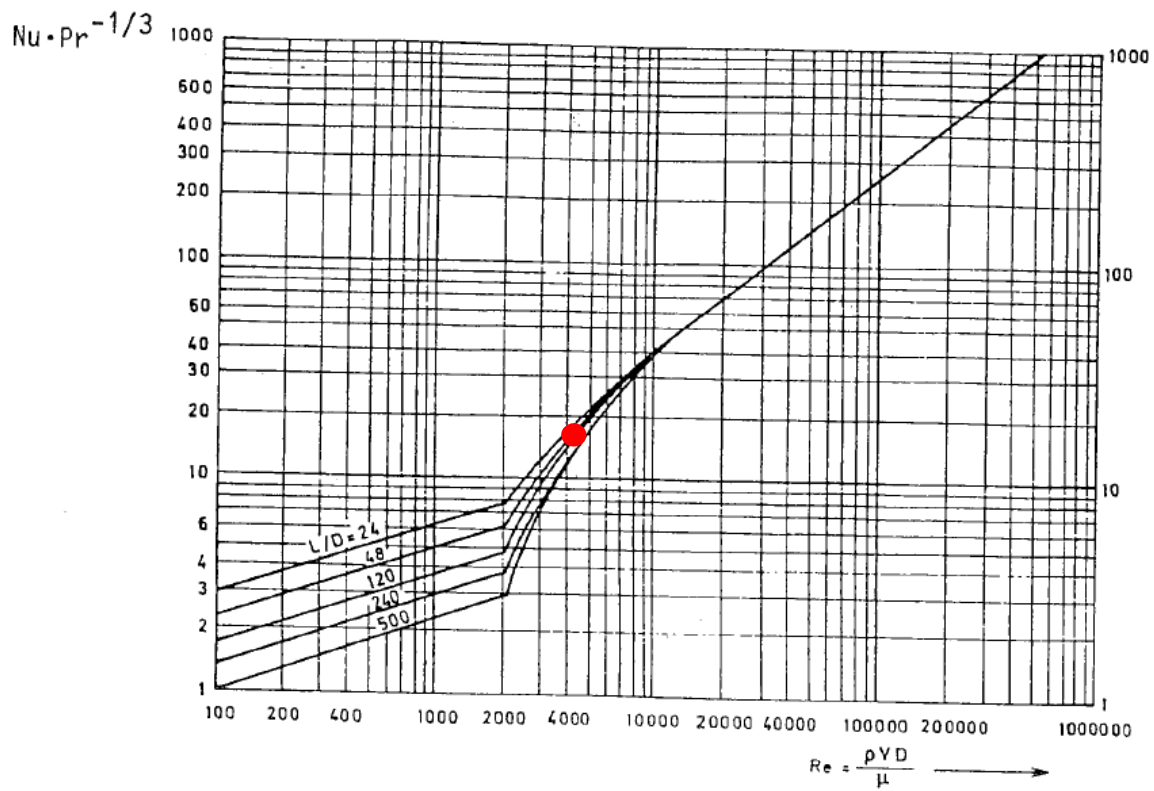


Figure 16: This figure shows the graphical correlations between Reynolds, Nusselt and Prandtl for forced convection. [42] These Nusselt and Prandtl numbers are the heat equivalents of respectively Sherwood and Schmidt, which are used in mass transfer. In this graph, Nusselt and Prandtl may be changed at any time by Sherwood and Schmidt. The red dot corresponds for the Reynolds number of 4257, a length (L) of 0.5 m and D of 3 mm.

Chapter 9. References

- [1] W. Bollens, Experimental and theoretical study of a small scale chlorate electrolyzer, Master of Science Thesis, Chalmers Technical University, **2010**
- [2] T. Maes, Current efficiency studies in chlorate electrolysis, Master of Science Thesis, University of Gothenburg, **2011**
- [3] P. K. Weissenborn, R. J. Pugh, Surface Tension and Bubble Coalescence Phenomena of Aqueous Solutions of Electrolytes, *Langmuir*, 11, 1422-1426, **1995**
- [4] B. V. Tilak, K. Viswanathan, C.G. Rader, On the Mechanism of Sodium Chlorate Formation, *J. Electrochem. Soc.*, **1981**
- [5] G. Marrucci, L. Nicodemo, Coalescence of gas bubbles in aqueous solutions of inorganic electrolytes, *Chemical Engineering Science*, **1976**
- [6] B. V. Tilak, K. Viswanathan, Chemical, Electrochemical, and Technical Aspects of Sodium Chlorate Manufacture, *J. Electrochem. Soc.*, **1984**
- [7] P. K. Weissenborn, R. J. Pugh, Surface Tension of Aqueous Solutions of Electrolytes: Relationship with Ion Hydration, Oxygen Solubility, and Bubble Coalescence, *Journal of Colloid and Interface Science*, **1996**
- [8] G. Kreysa, M. Kuhn, Modelling of gas evolving electrolysis cells. I. The gas voidage problem, *Journal of Applied Electrochemistry*, **1985**
- [9] J. Zahradník, M. Fialova, F. Kaštánek, K. D. Green, N. H. Thomas, The effect of electrolytes on bubble coalescence and gas holdup in bubble column reactors, *Trans IChemE*, Vol 73, Part A, 341-346, **1995**
- [10] P. T. Nguyen, M. A. Hampton, A. V. Nguyen, G. R. Birkett, The influence of gas velocity, salt type and concentration on transition concentration for bubble coalescence inhibition and gas holdup, *Chemical Engineering Research and Design* 90, 33-39, **2012**
- [11] B. S. Chan, Y. H. Tsang, A theory on bubble-size dependence of the critical electrolyte concentration for inhibition of coalescence, *Journal of Colloid and Interface Science* 286, 410-413, **2005**
- [12] H. Vogt, A hydrodynamic model for the ohmic interelectrode resistance of cells with vertical gas evolving electrodes, *Electrochimica Acta*, Vol. 26, No. 9, 1311-1317, **1981**
- [13] H. Vogt, The rate of gas evolution at electrodes - I. an estimate of the efficiency of gas evolution from the supersaturation of electrolyte adjacent to a gas-evolving electrode, *Electrochimica Acta*, Vol. 29, No. 9, 167-173, **1984**

- [14] A Nallet, R. A. Paris, *Bull. Soc. Chim. Fr.*, 488-494, **1956**
- [15] A. N. Campbell, E. M. Kartzmark, B. G. Oliver, The electrolytic conductances of sodium chlorate and of lithium chlorate in water and in water-dioxane, *Canadian Journal of Chemistry*, Vol. 44, 925-934, **1966**
- [16] A. N. Campbell, B. G. Oliver, Activities from vapor pressure measurements of lithium and of sodium chlorates in water and water-dioxane solvents, *Canadian Journal of Chemistry*, Vol. 47, 2671-2680, **1969**
- [17] R. H Perry, C. H. Chilton, S. D. Kirkpatrick, Perry's Chemical Engineers' Handbook, 4th edition. **1963**
- [18] A. Smolianski, H. Haario, P. Luukka, Numerical Study of Dynamics of Single Bubbles and Bubble Swarms, *Applied Mathematical Modeling*, 32(5), 641-659, **2008**
- [19] The Chlorate Manual, Kerr-McGee Chemical Group, **1972**
- [20] R. T. Cygan, The solubility of gases in NaCl brine and a critical evaluation of available data, Sandia national laboratories, **1991**
- [21] Clift, R., Grace, J. R., Weber, M. E.: *Bubbles, drops and particles*, Academic Press, New York, **1978**
- [22] L.J.J. Janssen, Effective solution resistivity in beds containing one monolayer or multilayers of uniform spherical glass beads, *Journal of Applied Electrochemistry* 30, 507-509, **2000**
- [23] N. V. S. Knibbs, H. Palfreeman, The theory of electrochemical chlorate and perchlorate formation, *Trans. Faraday Soc.*, 16, 402-433, **1920**
- [24] S. Ajdari, Modeling and Simulation of a Small Scale Chlorate Electrolyzer, Master of Science Thesis, Chalmers Technical University, **2011**
- [25] P. Byrne, Mathematical Modeling and Experimental Simulation of Chlorate and Chlor-alkali Cells, Doctoral Thesis, KTH Stockholm, **2001**
- [26] R. Wetind, Two-Phase Flows in Gas-Evolving Electrochemical Applications, Doctoral Thesis, KTH Stockholm, **2001**
- [27] B.V. Tilak, Electrolytic Sodium Chlorate Technology: Current Status, Electrochemical Society Proceedings, Vol. 99-21
- [28] B. Andersson, R. Andersson, L. Håkansson, M. Mortensen, R. Sudiyo, B. van Wachem, *Computational Fluid Dynamics for Engineers*, 8th ed, Gothenburg, Sweden
- [29] A. Cornell, Electrode Reactions in the Chlorate Process, Doctoral Thesis, KTH Stockholm, **2002**

- [30] L. Nylén, Influence of the electrolyte on the electrode reactions in the chlorate process, Doctoral Thesis, KTH Stockholm, **2008**
- [31] wetting angle formulas, <http://www.eng.utah.edu/~ljang/images/lecture-12.pdf>, <consulted on 2012-04-20>
- [32] C. E. Brennen, cavitation and bubble dynamics, <http://authors.library.caltech.edu/25017/4/chap1.htm>, Oxford university press, **1995**, <consulted on 2012-04-20>
- [33] B. V. Tilak, C.-P. Chen, Electrolytic sodium chlorate technology: current status, *Electrochemical Society*, 8-30
- [34] H.-J. Butt, K. Graf, M. Kappl, *Physics and Chemistry of Interfaces*, Wiley-VCH Verlag & Co. KGaA, **2003**
- [35] G. Marrucci, Rising Velocity of a Swarm of Spherical Bubbles, *Ind. Eng. Chem. Fundam.* 4, 224-225, **1965**
- [36] D. J. Nicklin, J. O. Wilkes, J. F. Davidson, Two phase flow in vertical tubes, *Trans. Inst. Chem. Eng.* 40, 61-68, **1962**
- [37] D. J. Nicklin, Two-phase bubble flow, *Chem. Eng. Sci.* 17, 693-702, **1962**
- [38] N. P. Brandon, G.H. Kelsall, S Levine, A. L. Smith, Interfacial electrical properties of electrogenerated bubbles, *J. Appl. Electrochem.* 15, 485-493, **1985**
- [39] V. S. J. Craig, Bubble coalescence and specific-ion effects, *Current opinion in Colloid Interface Sci.* 9, 178-184, **2004**
- [40] M. Tourwé, Massaoverdracht, cursus Artesis Hogeschool, **2010**
- [41] drawing by Johan Wanngård, **2011**
- [42] Graph: Nusselt Prandtl and Reynolds correlation for forced convection, http://www.chemeng.lth.se/ketf01/Arkiv/TP9_v%E4rmell.pdf, <consulted on 2012-07-19>
- [43] S. F. Jones, G. M. Evans, K. P. Galvin, Bubble nucleation from gas cavities – a review, *Advances in Colloid and Interface Science* 80, 27-50, **1999**
- [44] Lide, D.R., CRC Handbook of Chemistry and Physics, 90th edition, CRC Press, Boca Raton, FL, USA, p. 6-5., **2009**